

Grouting the tail void

Analysis of the tail void grouting
process at the North/South line

M. Vonk

Grouting the tail void

Analysis of the tail void grouting process at the North/South line

by

M. Vonk

to obtain the degree of Master of Science
at the Delft University of Technology,
to be defended publicly on Tuesday March 5, 2020 at 17:00.

Student number: 4238311

Thesis committee:	Dr. ir. W. Broere,	TU Delft, Chair
	Ir. K. J. Reinders,	TU Delft
	Ir. drs. R. E. P. de Nijs CEng,	TU Delft, Witteveen+Bos
	Ir. F. J. Kaalberg,	Witteveen+Bos

An electronic version of this thesis is available at <http://repository.tudelft.nl/>.

Abstract

To fight increasing traffic in city centres, tunnelling can be used to move traffic under the surface of the busy city. However, to prevent damage to the surrounding buildings, the settlements induced by the tunnelling should be kept to a minimum. This thesis researches the influence of the TBM tail void and its grouting process on the settlements.

To do so, the monitoring and TBM data from the North/South line in Amsterdam is used. The data of the settlements, grout pressures and grout volumes is searched for locations with sudden changes. For these locations, the development of the settlements as a function of the TBM movement is compared to find out if the changes in settlements are caused by the tail void. This turns out to be the case for half of the researched locations. Furthermore, the changes of the grout pressures measured in the tail void, and the volume injected grout volume are compared for these locations. An increase in injected grout volume shows to decrease the settlements induced by the tail void, while the pressure does not show a correlation with the settlements. Because only one sensor was used for the pressure measurements, the grout pressures are then compared for all sensors in the tail void. Again, no correlation is found between the grout pressures and the settlements. A side step in the research shows the development of the grout pressures in the tail void. During the boring process the grout pressures fluctuate. During the boring and forward movement of the TBM the tail void is injected with grout and the grout pressures in the tail void increase. During the ring building phase, this grouting stops and the grout pressures start to dissipate. The amount of dissipation is influenced by the permeability of the surrounding soil. With the help of DIANA FEM software, the influence of the tail void on the total settlements is investigated. The calculations show that a different grouting behaviour caused a change of only 4 mm in total settlements.

Concluding, as long as the pressures in the tail void stay above the soil pressure the tail void can be filled with grout. The injected grout volume will fill the tail void, preventing the soil from moving into the tail void and with that minimising the settlements at the surface.

Preface

Before you lies the thesis concludes the Master of Science program in Geo-engineering at Delft University of Technology. I am thankful that I could do the thesis at Witteveen+Bos and could use their data and expertise. I also would like to express my gratitude towards Wout, Kristina, Richard and Frank of the graduation committee for all the help during my research, without you this would not have been possible.

Then I would like to thank the colleagues at Witteveen+Bos for the input and distractions during the coffee and lunch breaks, especially Zhekang with all his help in developing the DIANA model.

Finally, I would like my friends who were graduating at the same times and understood the struggles of writing a thesis. A special thanks to Linda who was not graduating with me but did have to live with me during the writing of the thesis, for all the emotional support and patience during my graduation.

"Uiteindelijk komt alles goed. Als het nog niet goed is, is het ook nog niet uiteindelijk."

M. Vonk

Den Haag, February 2020

Contents

List of Figures	ix
1 Introduction	1
1.1 Relevance of this research.	1
1.2 Research goal and scope	1
1.2.1 Research questions	1
1.3 Methods	1
2 Literature Study	3
2.1 Tunnel boring.	3
2.2 Settlements	3
2.2.1 Development of the settlements during the TBM passage	3
2.2.2 Settlement trough	4
2.3 Development of the grout pressures in the tail void	5
2.3.1 Grout injection.	5
2.3.2 Grout consolidation due to fluid loss.	5
2.4 Tail void injection tests	6
3 North/South line	9
3.1 TBM	10
3.2 Monitoring concept.	11
3.3 Frozen canopy	11
4 Total settlements and grouting	13
4.1 Methods	13
4.1.1 Settlements	13
4.1.2 Grout pressure	13
4.1.3 Grout Volume	14
4.2 RT1	15
4.2.1 Settlements	15
4.2.2 Grout pressure	16
4.2.3 Grout volume	17
4.2.4 Subsurface	18
4.3 RT4	19
4.3.1 Settlements	19
4.3.2 Grout pressure	20
4.3.3 Grout volume	21
4.3.4 Subsurface	22
4.4 Discussion	22
5 Development of the settlements during the TBM passage	25
5.1 Zone of influence	25
5.2 The normalised settlement development curve	27
5.3 Average settlement curve	28
5.4 Settlement development at zones of interest	29
5.4.1 RT1 West zone 1	29
5.4.2 RT1 West zone 2	31
5.4.3 RT1 West zone 3	33
5.4.4 RT1 East zone 1	34
5.4.5 RT1 East zone 2	35
5.4.6 RT1 East zone 3	36

5.4.7	RT4 West zone 1	38
5.4.8	RT4 West zone 2	40
5.4.9	RT4 West zone 3	41
5.4.10	RT4 East	43
5.5	Discussion	44
6	Grout- and soil pressures in the tail void	47
6.1	Methods	47
6.2	RT1 zone 2	47
6.2.1	RT1W2	48
6.2.2	RT1E2	50
6.2.3	RT1E3	50
6.2.4	RT4W	52
6.3	Discussion	52
7	Dissipation of the grout pressures during TBM standstill	53
7.1	Methods	53
7.2	Dependency of the grout pressure dissipation on the surrounding soil	53
7.3	Discussion	53
8	Finite Element Model validation	55
8.1	Methods	55
8.2	Varying the grout pressures	55
8.3	Discussion	56
9	Discussion and Conclusions	59
9.1	Main findings	59
9.2	Discussion	60
9.3	Conclusions.	60
10	Recommendations	63
	Bibliography	65

List of Figures

2.1	Settlements induced by various TBM components (Vu et al. 2016).	4
2.2	Settlements induced by tunnelling (Haji 2017) after (Attewell et al. 1986)	4
2.3	Distribution of grout pressure at a distance from the injection point (Babendererde 1999).	5
2.4	1D schematic representation of the grout consolidation process (Dias and Bezuijen 2015).	6
2.5	Schematic view of the North/South line TBM(left) and the test shield(right).	6
2.6	Overview of the tail void test location.	7
2.7	Exposed grout which was injected under a pressure higher than the soil pressure.	7
3.1	Trajectory of the N/S line bored tunnel (COB)	9
3.2	TBM tail and grout pressure sensors	10
4.1	Example of a plot using the grout pressures per ring(left) and averaged over 5 rings(right).	14
4.2	Example of a plot using the grout volumes per ring (left) and averaged over 5 rings (right).	15
4.3	Settlement profile of the RT1 West trajectory divided in sections based on the settlements.	15
4.4	Settlement profile of the RT1 East trajectory divided in sections based on the settlements.	16
4.5	Measured grout pressures in the tail void of the RT1 West trajectory	16
4.6	Measured grout pressures in the tail void of the RT1 East trajectory	17
4.7	Used grout volumes during the boring of the RT1 West trajectory.	17
4.8	Used grout volumes during the boring of the RT1 East trajectory.	18
4.9	Geotechnical profile of tunnel section RT1 and zones of interest.	18
4.10	Settlement profile of the RT4 West trajectory divided in sections based on the settlements.	19
4.11	Settlement profile of the RT4 East trajectory divided in sections based on the settlements.	20
4.12	Measured grout pressures in the tail void of the RT4 West trajectory	20
4.13	Measured grout pressures in the tail void of the RT4 East trajectory(gaps are due to missing data).	21
4.14	Used grout volumes during the boring of the RT4 West trajectory.	21
4.15	Used grout volumes during the boring of the RT4 East trajectory(gaps are due to missing data).	22
4.16	Geo-technical profile of tunnel section RT4 and points of interest.	22
4.17	Scatter plot of the grout volumes injected in the tail void(top x axis) and the grout pressures in the tail void (bottom x axis) against the settlements.	23
5.1	Example of determination of the point of inflection.	26
5.2	Graphically image of inflection points at different tunnel depths	26
5.3	Settlement development curve comparison RT1 West zone 2.	27
5.4	Normalised settlement development curve comparison RT1 West zone 2.	27
5.5	Normalised settlement development curve comparison RT1 West zone 2.	28
5.6	Measurements of RT1 West between 203m and 211m.	29
5.7	Measurements of RT1 West between 203m and 211m with the influence of the size of the window.	29
5.8	Comparison of the average settlement development curves of RT1 West zone 1.	30
5.9	Comparison of the normalised average settlement development curves of RT1 West zone 1.	30
5.10	Comparison between the regions just before and after zone 2 in RT1West	31
5.11	Zoomed comparison between the regions just before and after zone 2 in RT1West.	32
5.12	Normalised comparison between the regions just before and after zone 2 in RT1West.	32
5.13	Comparison of the average settlement development curves of RT1 West zone 3.	33
5.14	Comparison of the normalised average settlement development curves of RT1 West zone 3.	33
5.15	Comparison of the average settlement development curves of RT1 East zone 1.	34
5.16	Comparison of the normalised average settlement development curves of RT1 East zone 1.	34
5.17	Comparison of the average settlement development curves of RT1 East zone 2.	35
5.18	Comparison of the normalised average settlement development curves of RT1 East zone 2.	35
5.19	Comparison of the normalised average settlement development curves of RT1 East zone 2.	36

5.20	Comparison of the average settlement development curves of RT1 East zone 3.	36
5.21	Comparison of the normalised average settlement development curves of RT1 East zone 3. . . .	37
5.22	Comparison of the normalised average settlement development curves of RT1 East zone 3. . . .	37
5.23	Comparison of the average settlement development curves of RT4 West zone 1.	38
5.24	Comparison of the normalised average settlement development curves of RT4 West zone 1. . . .	38
5.25	Comparison of the normalised average settlement development curves of RT4 West zone 1. . . .	39
5.26	Comparison of the average settlement development curves of RT4 West zone 2.	40
5.27	Comparison of the normalised average settlement development curves of RT4 West zone 2. . . .	40
5.28	Comparison of the normalised average settlement development curves of RT4 West zone 2. . . .	41
5.29	Comparison of the average settlement development curves of RT4 West zone 3.	41
5.30	Comparison of the normalised average settlement development curves of RT4 West zone 3. . . .	42
5.31	Comparison of the normalised average settlement development curves of RT4 West zone 3. . . .	42
5.32	Comparison of the average settlement development curves of RT4 East.	43
5.33	Comparison of the normalised average settlement development curves of RT4 East.	43
5.34	Comparison of the normalised average settlement development curves of RT4 East.	44
5.35	Scatter plot of the grout pressures in the tail void (left y axis) and the grout volumes injected in the tail void (right y axis) against the distance between the front of the TBM and point of measurement at the moment the total settlements are reached.	45
6.1	Polar representation of the grout pressures in the tail void at the beginning of the boring phase of ring 130 at the RT1 West trajectory.	49
6.2	Polar representation of the grout pressures in the tail void at the beginning of the ring building phase of ring 130 at the RT1 West trajectory.	49
6.3	Polar representation of the grout pressures in the tail void at the end of the ring building phase of ring 130 at the RT1 West trajectory.	49
6.4	Polar representation of the grout pressures in the tail void at the beginning of the boring phase of ring 143 at the RT1 West trajectory.	49
6.5	Polar representation of the grout pressures in the tail void at the beginning of the ring building phase of ring 143 at the RT1 West trajectory.	49
6.6	Polar representation of the grout pressures in the tail void at the end of the ring building phase of ring 143 at the RT1 West trajectory.	49
6.7	Polar representation of the grout pressures in the tail void at the beginning of the boring phase of ring 234 at the RT1 East trajectory.	50
6.8	Polar representation of the grout pressures in the tail void at the beginning of the ring building phase of ring 234 at the RT1 East trajectory.	50
6.9	Polar representation of the grout pressures in the tail void at the end of the ring building phase of ring 234 at the RT1 East trajectory.	50
6.10	Polar representation of the grout pressures in the tail void at the beginning of the boring phase of ring 252 at the RT1 East trajectory.	50
6.11	Polar representation of the grout pressures in the tail void at the beginning of the ring building phase of ring 252 at the RT1 East trajectory.	50
6.12	Polar representation of the grout pressures in the tail void at the end of the ring building phase of ring 252 at the RT1 East trajectory.	50
6.13	Polar representation of the grout pressures in the tail void at the beginning of the boring phase of ring 287 at the RT1 East trajectory.	50
6.14	Polar representation of the grout pressures in the tail void at the beginning of the ring building phase of ring 278 at the RT1 East trajectory.	50
6.15	Polar representation of the grout pressures in the tail void at the end of the ring building phase of ring 278 at the RT1 East trajectory.	50
6.16	Polar representation of the grout pressures in the tail void at the beginning of the boring phase of ring 375 at the RT1 East trajectory.	51
6.17	Polar representation of the grout pressures in the tail void at the beginning of the ring building phase of ring 375 at the RT1 East trajectory.	51
6.18	Polar representation of the grout pressures in the tail void at the end of the ring building phase of ring 375 at the RT1 East trajectory.	51

6.19 Polar representation of the grout pressures in the tail void at the beginning of the boring phase of ring 426 at the RT1 East trajectory.	51
6.20 Polar representation of the grout pressures in the tail void at the beginning of the ring building phase of ring 426 at the RT1 East trajectory.	51
6.21 Polar representation of the grout pressures in the tail void at the end of the ring building phase of ring 426 at the RT1 East trajectory.	51
6.22 Polar representation of the grout pressures in the tail void at the beginning of the boring phase of ring 88 at the RT4 West trajectory.	52
6.23 Polar representation of the grout pressures in the tail void at the beginning of the ring building phase of ring 88 at the RT4 West trajectory trajectory.	52
6.24 Polar representation of the grout pressures in the tail void at the end of the ring building phase of ring 88 at the RT4 West trajectory trajectory.	52
6.25 Polar representation of the grout pressures in the tail void at the beginning of the boring phase of ring 140 at the RT4 West trajectory.	52
6.26 Polar representation of the grout pressures in the tail void at the beginning of the ring building phase of ring 140 at the RT4 West trajectory.	52
6.27 Polar representation of the grout pressures in the tail void at the end of the ring building phase of ring 140 at the RT4 West trajectory.	52
6.28 Polar representation of the grout pressures in the tail void at the beginning of the boring phase of ring 230 at the RT4 West trajectory.	52
6.29 Polar representation of the grout pressures in the tail void at the beginning of the ring building phase of ring ring 230 at the RT4 West trajectory.	52
6.30 Polar representation of the grout pressures in the tail void at the end of the ring building phase of ring ring 230 at the RT4 West trajectory.	52
7.1 Grout pressures during drilling and stand still in clay(here the groundwater pressure under the bottom of the graph and is 250 kPa	54
7.2 Grout pressures during drilling and stand still in sand	54
8.1 Overview of the FEM model.	56
8.2 Inner soil of the FEM model.	56
8.3 Overview of the settlements induced by the FEM model at 400kPa	57
8.4 Overview of the FEM model	57

Introduction

1.1. Relevance of this research

To fight increasing traffic in city centres, tunnelling can be used to move, at least a part of, the traffic under the surface of the busy city. This keeps cities accessible and liveable. While tunnelling under the city limits nuisance and disturbance induced by construction works at the surface, it will cause settlements at the surface. These settlements can lead to damage to existing buildings. A better understanding of the caused settlements makes it possible to either limit them or ensure they arise in more favourable locations, limiting damages to buildings.

A part of these settlements are caused by the soil closing into the tail void. This tail void is filled with liquid grout to prevent the soil from closing in. Dijk van and Kaalberg (1998) started with the idea to improve the grouting process in such a way that tail void is supported by balancing the soil stress, minimising the deformations of the tunnel elements and the surrounding soil. This idea was further researched by the Dutch Centre of Underground Research (CUR) in their K100 and L520 reports. Hereafter Bezuijen and Bakker (2008); Bezuijen and Talmon (2008, 2003); Dias and Bezuijen (2015, 2017) continued this line of thought in their research, mainly focusing on the rheology of the grout and the fluctuations in the grout pressures.

1.2. Research goal and scope

The goal of this thesis research is to gain a better understanding of the settlements induced by the tail at the rear of the Tunnel Boring Machine (TBM). Main focus is the correlation between the tail void injection process and the settlements induced at surface level. During this research, data from the TBM drilling process and the monitoring data, both gathered during the North-South line project in Amsterdam is used.

1.2.1. Research questions

Main question: *To what extend is the tail void behind the TBM responsible for the settlements and does the grouting of this tail void reduce these settlements?*

Sub questions:

- *How do the settlements develop during the passing of the TBM and which part of the settlements is affected by the tail void?*
- *Can a relation be found between the injected grout volumes and the settlements induced by the tail void?*
- *Can a relation be found between the grout pressures and the settlements induced by the tail void?*
- *How do the grout pressures develop over time i.e. do they dissipate when grout injections stops?*

1.3. Methods

To find a relation between the grouting processes and the settlements, data of the Amsterdam North/South line project is analysed. TBM data and data from the surrounding soil are compared to find correlations between tail void grouting process and the settlements. The data is first searched for sudden changes in

settlements along the tunnel trajectory. When these are located, an attempt is made to explain the sudden changes by using the data from the drilling process. Then, a method is developed to isolate the settlements induced by the tail void. These are checked for relations with the grouting parameters. Finally, a Finite Element Model(FEM) is used to check the influence of the tail void on the total settlements numerically.

2

Literature Study

In this chapter, a literature study is presented around the subject of settlements induced by TBM tunnelling, particularly focusing on the effects of the tail void grouting. First, paragraph 2.1 explains the different tunnel boring techniques. In paragraph 2.2, a distinction between settlements induced by different parts of the tunnelling process is presented. The variation of the grout pressures in the tail void is explained in paragraph 2.3. Finally, paragraph 2.4 explains the tail void injection tests executed especially for the North/South line.

2.1. Tunnel boring

This section is based on: Reinders (2018) and Möller (2006).

Tunnel boring creates the possibility for building tunnels in locations where cut-and-cover and immersed tunnelling is not possible, such as densely populated areas and deep water crossings. Multiple tunnel boring techniques exist, which can be divided in two types of tunnelling: open- and closed face tunnelling. During open face tunnelling, the tunnel face is not supported. In closed face tunnelling however, compressed air, slurry or an earth pressure balance control is used to support the tunnel face. As for the drilling of the North/South line, a closed face slurry TBM was used, this thesis only focuses on that type of tunnel boring.

The slurry TBM is assembled in a starting shaft from where it starts building the tunnel. At the face of the TBM, a rotating cutter wheel excavates the soil in front of the face, while jacks at the back of the TBM push against a starting block and move the TBM forward. When the jacks are fully extended, they are retracted so the first ring can be build. The ring consists of multiple segments, forming the final lining of the tunnel. This process of pushing forward and building new tunnel rings is repeated until the tunnel is completed.

In front of the TBM, a bentonite slurry is kept under pressure to support the tunnel face from caving in. While soil is excavated by the cutting wheel it is mixed with the slurry. This mix of soil and slurry is pumped through the TBM and tunnel to the starting shaft, where a slurry treatment plant splits the excavated soil from the slurry, whereafter the slurry is pumped back to the front of the TBM.

At the back of the TBM, measurements are taken to prevent settlements at the surface and stabilise the tunnel lining. As the ring building process takes place inside the shield of the TBM, the excavated diameter is bigger than that of the final lining. This forms a so-called tail void between the outer ring surface and the surrounding soil. To prevent soil moving into the tail void and causing settlements at the surface, the tail void is filled with grout during the forward movement of the TBM.

2.2. Settlements

The role of the TBM is not only to excavate soil to make space for the tunnel, but also to support adjacent soil to prevent deformation and settlements.

2.2.1. Development of the settlements during the TBM passage

The different phases of the surface settlements can be related to the various TBM components (figure 2.1 (Kaalberg and Hentschel 1998; Vu et al. 2016)).

The first phase of settlements are those that occur at-, and in front of the tunnelling face. These settlements can be controlled by the use of the correct TBM and face pressures (Kaalberg and Hentschel 1998).

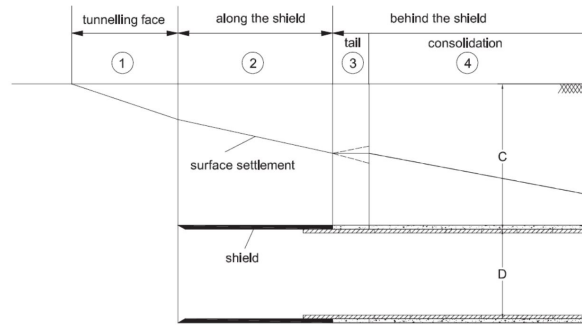


Figure 2.1: Settlements induced by various TBM components (Vu et al. 2016).

The settlements are induced by the tendency of the soil to move towards the cavity in front of the TBM. This movement can be reduced by keeping the front pressure high enough to prevent the soil to collapse into the excavation chamber. However, the pressure should not be too high, as this can lead to deformations and a possible blow-out. During a blow-out, the front pressure is so high that the slurry finds a way to the surface, making it impossible to maintain front pressure which leads to a collapse of the tunnel face (Vu et al. 2016).

The next phase of the settlements is induced along the shield of the TBM. The tapered shape of the TBM shield and the tendency of the soil to move towards the shield, are the cause of this volume loss (Vu et al. 2016). However, it is assumed that the solid does not fully contract towards the TBM shield. The slurry at the TBM face and the grout at the TBM tail is expected to migrate along the TBM shield. This assumption was confirmed by the discovery of grout residue at the shield of the TBM that bored the 2nd Heijenennoord tunnel in the Netherlands (Bezuijen et al. 2011). The pressures of these fluids should be able to stop the soil from moving towards the shield (Bezuijen and Bakker 2008; Bezuijen and Talmon 2008). This theory is further supported by the findings of Festa (2015) who discovered that the drag forces along the shield were far lower than expected without fluid around the TBM. The third phase of settlements are caused by the tail void at the back of the TBM. This tail void is filled with grout supporting the surrounding soil. When the pressure of this grout falls below the soil pressure of the surrounding soil, the cavity will contract which causes settlements at the surface. Theoretically an increase of the grout pressure can lead to a negative volume loss and therefore even decrease the settlements at the surface (Vu et al. 2016).

In the final phase of settlements, the change in soil stresses around the tunnel cause consolidation of the soil. This leads to long-term settlements which can account for 30-90% of the total settlements (Vu et al. 2016).

2.2.2. Settlement trough

In 1969, Peck (1969) introduced a Gaussian curve that could fit the settlement trough induced by a tunnel. The volume of this trough is assumed to be the same as the volume of the soil loss around the tunnel. Figure 2.2 shows this Gaussian fit in the x direction and the development of the settlement during the TBM passage in the y direction.

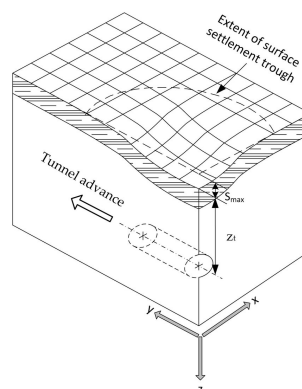


Figure 2.2: Settlements induced by tunnelling (Haji 2017) after (Attewell et al. 1986)

2.3. Development of the grout pressures in the tail void

To understand the induced settlements, a better understanding of the build up- and dissipation of the grout pressure in the tail void is required. In this chapter, multiple aspects of the pressure changes are considered.

2.3.1. Grout injection

The best way to prevent the settlements due to the tail void would be keeping a constant grout pressure in the tail void stopping the surrounding soil from closing in towards the lining. However, a constant pressure is difficult to obtain due to the limited amount of grout injection points. The grout pressure at the injection points is higher than at a distance from these points, where the pressure drops due to the friction along the soil and lining and, the yield strength of the grout. The yield strength even increases due to the loss of fluid, reducing the flow capacity to the surrounding soil (Babendererde 1999) (figure 2.3). The concept of the fluid loss is further explained in paragraph 2.3.2.

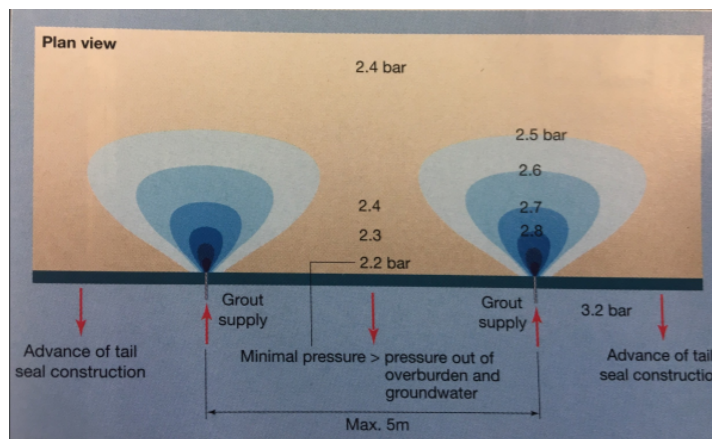


Figure 2.3: Distribution of grout pressure at a distance from the injection point (Babendererde 1999).

2.3.2. Grout consolidation due to fluid loss

Since the grout pressure is higher than the pore water pressure in the surrounding soil, water is expected to migrate from the grout into the soil. Research of Bezuijen and Talmon (2003) and Dias and Bezuijen (2015) shows that the grout pressure in the tail void decreases during stand still of the TBM (during the ring building), indeed implying the fluid loss. This loss of fluid is also called the consolidation of the grout. A big factor in the consolidation rate of the grout is the permeability of the surrounding soil. The permeability of the soil determines the rate of outflow. Therefore a very impermeable soil like a clay could stop the grout from consolidating at all (Vu et al. 2016). As the consolidation goes on the cement of the grout will block the pores and decrease the consolidation rate.

Furthermore, the papers of Bezuijen and Talmon (2003) and Dias and Bezuijen (2015) illustrate that during this consolidation, the grout mixture becomes thicker (the cement-water ratio increases, decreasing the viscosity of the mixture). The small particles in the grout will clog the surrounding soil during the outflow of the water, forming a filter cake to form on the soil-grout interface (figure 2.4). This filter cake will have a lower permeability, causing the discharge to decrease. Therefore, the pressure drop slows down until the outflow becomes negligible and the pressure becomes constant. This state can be compared with the surrounding soil having a low permeability to begin with and the pressure drop should not be occurring.

Finally, the consolidation process causes the vertical pressure gradient in the tail void to decrease. As the pressure difference between the grout and the pore water at the bottom of the tail void is larger than at the top of the tail void, there is a bigger outflow at the bottom than at the top of the tail void. In combination with the different responses of the soil at different heights in the annulus causes the void to increase at the sides while it decreases in size at the bottom at the top of the borehole (Dias and Bezuijen 2017).

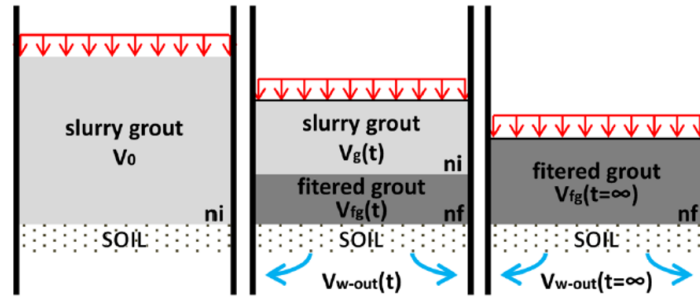


Figure 2.4: 1D schematic representation of the grout consolidation process (Dias and Bezuijen 2015).

2.4. Tail void injection tests

Before the North/South line was constructed, tests were developed. The goal of these tests was to achieve a better understanding of the tail void injection process and to test an innovative grout injection system, specially developed for the North/South line. Figure 2.6 shows an overview of the test location. The designed tests used a scaled-down version of the TBM, only containing a shield and the tail void behind it. The shields were placed in a pressurised tank filled with sand and water. The test shield was pushed through the sand and tunnel linings are installed inside the shield, just like in a normal TBM. During the forward movement of the shield, the created tail void was filled with grout. Figure 2.5 shows a schematic view of the test shield and the real TBM.

The tests showed that when the grout pressure was maintained at a level above the soil pressure and new grout was constantly injected during the movement of the shield, the tail void was became well filled (figure 2.7). When the test was performed without constant grout injection during shield movement the grout pressures dropped below the soil pressure and the tail void was not completely filled. This can be attributed to the sand moving into the tail void. Thus, for an optimal filling of the tail void, the grout pressure should exceed the soil pressure during the forward movement of the TBM.

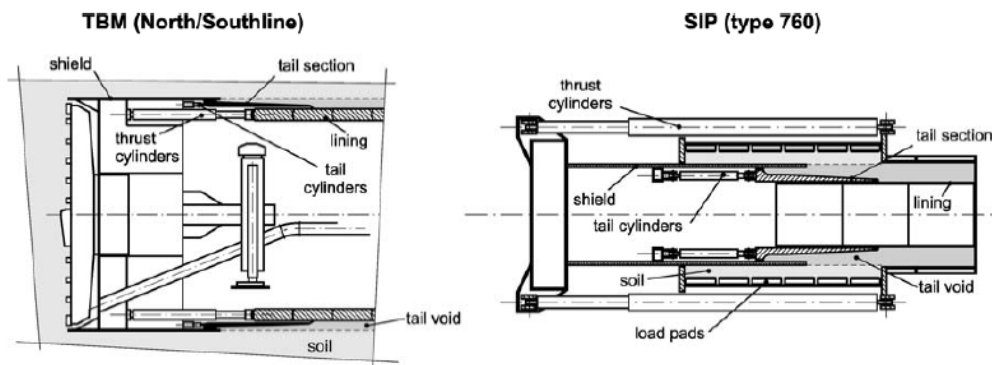


Figure 2.5: Schematic view of the North/South line TBM(left) and the test shield(right).

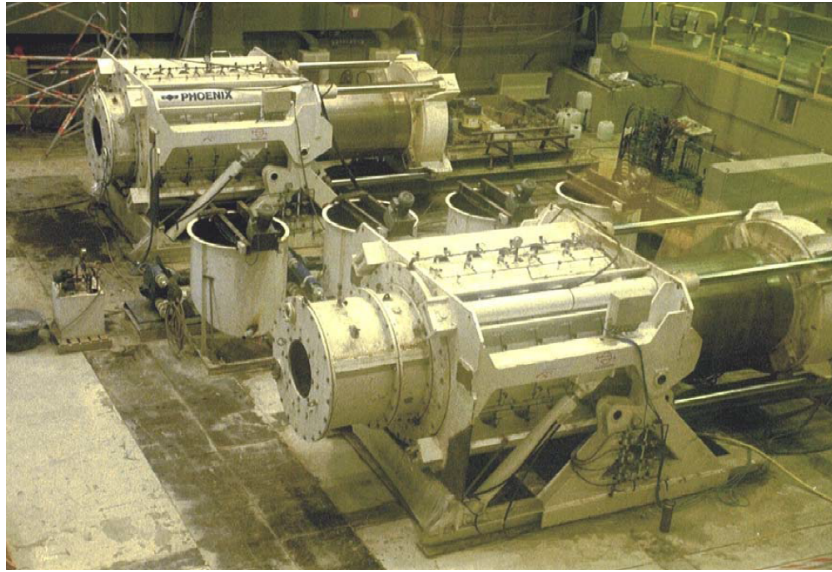


Figure 2.6: Overview of the tail void test location.



Figure 2.7: Exposed grout which was injected under a pressure higher than the soil pressure.

3

North/South line

This chapter is based on: (Kaalberg et al. 2003) and (COB 2016).

To fight the increasing population and traffic in the city centre of Amsterdam, the North/South metro line was constructed. Earlier construction of metro lines used a cut and cover technique, requiring demolition of many historic buildings and causing a lot of disturbance in the centre. This deconstruction and disturbance resulted in a public opposition for the further expansion of the Amsterdam metro system. To overcome this problem, the part of the North/South line under the old city centre was built using a TBM. The bored trajectory of the North/South line runs from Amsterdam Central Station in the North, to station Europaplein (called Scheldeplein at the moment of boring) in the South. The distance between those stations is 3.6 km, excluding the stations this is 3.1 km of tunnel, resulting in a total bored distance of 6.2km.

In 2010 the boring started at the Amsterdam Central Station. The original plan was to continue drilling towards the south, but due to problems during the construction of station Vijzelsgracht the TBM shields were 'parked' at station Rokin. The inner works of the TBMs were moved all the way south to station Scheldeplein, to start boring in the northern direction. The boring was finalised at the end of year 2012.

The tunnel trajectory is divided in 4 trajectories (RT1-RT4, figure 3.1), consisting of an Eastern and a Western tube. The trajectory runs mostly through sand, except for a part of the RT3 trajectory where the tunnel runs through the Eemclay. The trajectory follows the streets as much as possible to minimise the effects on the surrounding buildings. This guideline even resulted in stacking the two tubes at the end of the RT4 trajectory to follow the narrow Scheldestraat.

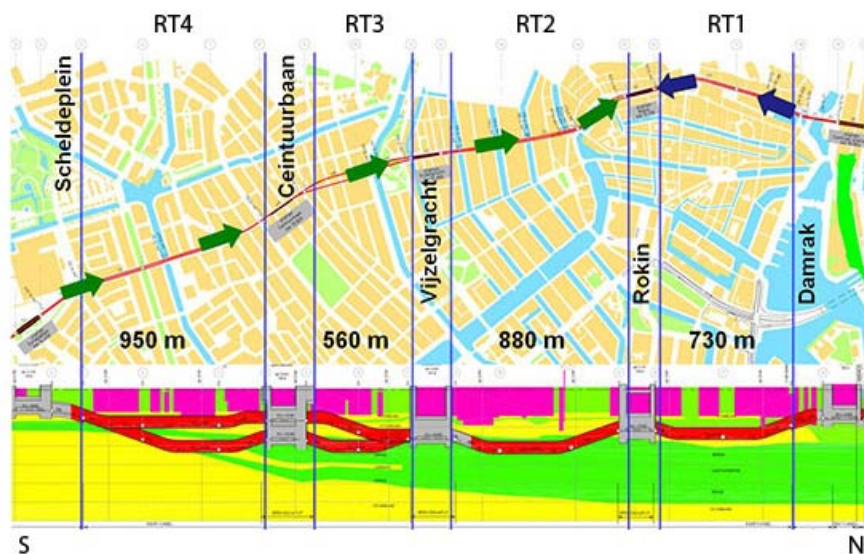


Figure 3.1: Trajectory of the N/S line bored tunnel (COB)

3.1. TBM

This section is based on: (Kaalberg and Hentschel 1998) and (Kaalberg et al. 2011).

The TBMs of the North/South line are specially designed to operate in the difficult conditions brought by boring underneath the city centre. First, the TBM encountered regular changing geological conditions of soft soils and needed to bore through the 1.5m thick D-walls of the reception shafts. The developed cutter wheel was kept relatively open to stop the cohesive soils from clogging in front of it and flush away easily. Furthermore the cutter wheel was equipped with strong 12" double disk cutters to be able to cut through the D-walls.

Secondly the tracks follow the street pattern which meant not only that the TBM had to be able to turn around tight corners but also that the tubes have to be close to each other to fit underneath the narrow street pattern. The TBM was kept relatively short (only 7.9 meter long) to keep the minimum corner radius at only 190 meter.

Finally, a low volume loss needed to be realised to limit the damage to imponderables. Research of Kaalberg et al. (2006) showed that piles of nearby buildings could only be passed at a distance of 0.5D if the volume loss was kept under 0.5%. The shorter length of the TBM, helped reaching this goal as the shorter tapering allowed less soil to move towards the TBM. Furthermore, the Integral Boring Control System (IBCS) was implemented, enabling TBM operators to monitor the reaction of the soil to the tunnel boring. This system was fed with the surface monitoring data (see paragraph 3.2) and with the data from the TBM itself. This makes it possible to control the face pressures very precisely, something that has been proven to work during the boring of the North/South line. More interesting for this thesis is that the grout pressures in the tail void were also measured and sent to the IBCS during boring. The pressures were measured by 6 sensors attached to the back of the TBM (figure 3.2) and saved every 10 seconds.

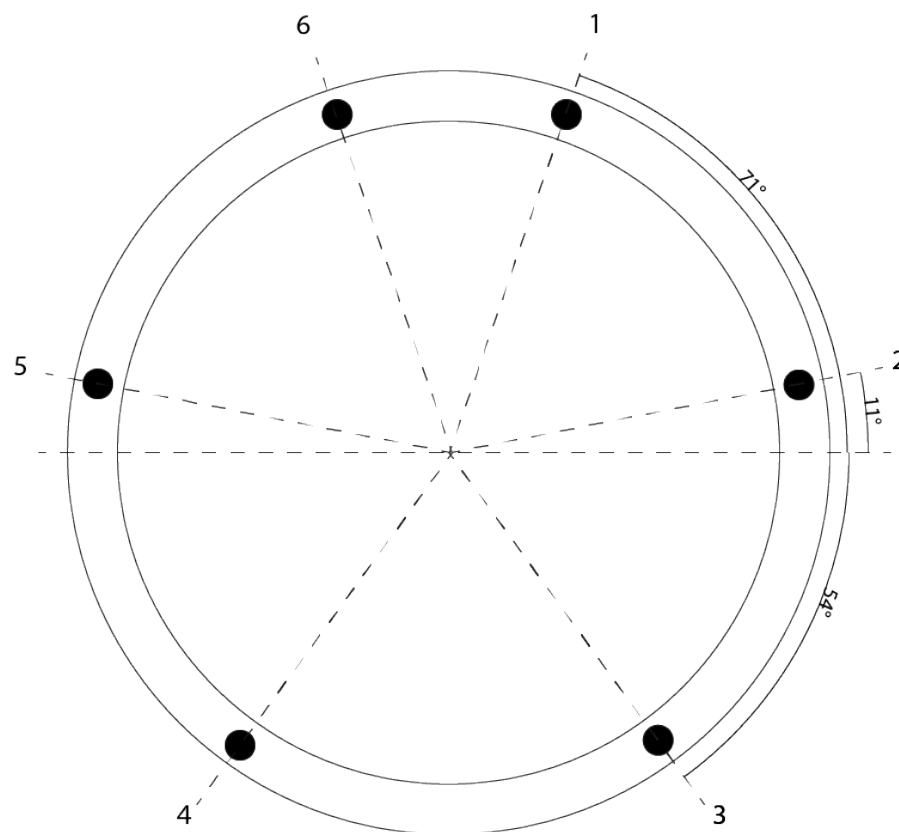


Figure 3.2: TBM tail and grout pressure sensors

3.2. Monitoring concept

This section is based on: (Cook et al. 2007) and (COB 2016).

At the time of the project execution, the monitoring contract was one of the biggest in Europe. Due to the historic buildings adjacent to the construction site, a detailed monitoring of the movements of both the soil and the buildings was needed. To keep the disruption to the urban environment as low as possible and to automatise the measurements, Robotic Total Stations (RTS) performed the measurements above ground. The 74 RTSs took readings from 7500 prisms on the buildings, bridges and quay walls. For this thesis, the additional measurements above the tunnel axis are used. Above the tunnel axis, the road pavement was used as a reflector meaning that the instalment of prisms was not needed. The maximum distance between two points of measurements was 2 meters, and the measurements were performed every hour. The frequency of the other measurements was adapted to the location of the TBM.

3.3. Frozen canopy

This section is based on: (Kaalberg et al. 2011).

At the beginning of the RT1 trajectory close to the Amsterdam Central Station, the tunnel starts relatively shallow in very soft soils. In these soft soils, a historic quay wall is located, founded on wooden piles. Due to the old age of the quay wall, the exact depth of the wooden piles was unknown. Therefore, encountering the wooden piles with the TBM formed a significant risk. To overcome these problems, it was decided to freeze the soil above the TBM at that location. The frozen soil formed a canopy above the TBM, enabling the TBM to cut the wooden piles. Furthermore, the canopy allowed higher face pressures and provided a reliable airtight cover for the entry of the working chamber.

4

Total settlements and grouting

Sudden changes in the settlements along the tunnel trajectory indicate either a change in the geology or in the TBM behaviour. Possible changes in TBM behaviour are a change of the front pressure, the grout pressure or the used grout volumes. This chapter looks at the locations with sudden changes in settlements and compares these with the grouting behaviour and the local lithology. The development of the settlements of these locations are further analysed in chapter 5.

4.1. Methods

First, the total settlements are checked for sudden changes. The locations of these sudden changes in settlements, the measured grout pressures and the used grout volumes are indicated. Secondly, these locations are compared with the injected grout pressure and its volume. Finally, the lithology of these locations is checked to rule out a sudden change as a cause for the change in settlements.

4.1.1. Settlements

The settlements above the tunnel axis are measured using reflectorless measurements made by robotic total stations (chapter 3). The measurement data contains the X, Y and Z coordinates of the measurement point at the time of measurement. To convert this data to absolute settlements, the first Z measurement of every location is subtracted from the rest of the measurements. Hereafter, the absolute settlements for all of the measurement points along the boring axis are combined to create a visualisation of the total settlements along the boring axis.

4.1.2. Grout pressure

The easiest way to compare the used grout pressures with the settlement data is to plot them together in one graph along the drilling trajectory. However, the moments of TBM standstill during the ring building process makes this difficult as during such moments, different grouting pressures are measured on the same location. Because the effect of minimum and maximum pressures is not known, it is chosen to plot the maximum, average and minimum values of the grouting pressure per ring. This is done for only 1 of the 6 sensors because all six sensors give comparable results. During the boring phase, the grout pressure reaches the maximum value, while during the ring building phase the injection of the tail void stops and the pressure drops, hence the minimum pressure. The average grout pressure is added because the time spent on ring building and boring varies.

Figure 4.1 shows an example of a plot of the minimum, maximum and, average grout pressures in the tail void. In the left figure, the pressures per ring are visualised. The graph shows that the grouting pressures fluctuate strongly, making it difficult to distinguish the three pressure lines and to recognise patterns. To overcome this problem, and since the grout stays liquid over the boring of more than one ring, a running average over 5 rings is used. The right side of figure 4.1 shows the results for the running average of the grout pressures. It can be seen that the maximum, minimum and, average lines are much easier to distinguish. Also the trends in the graphs appear clearer.

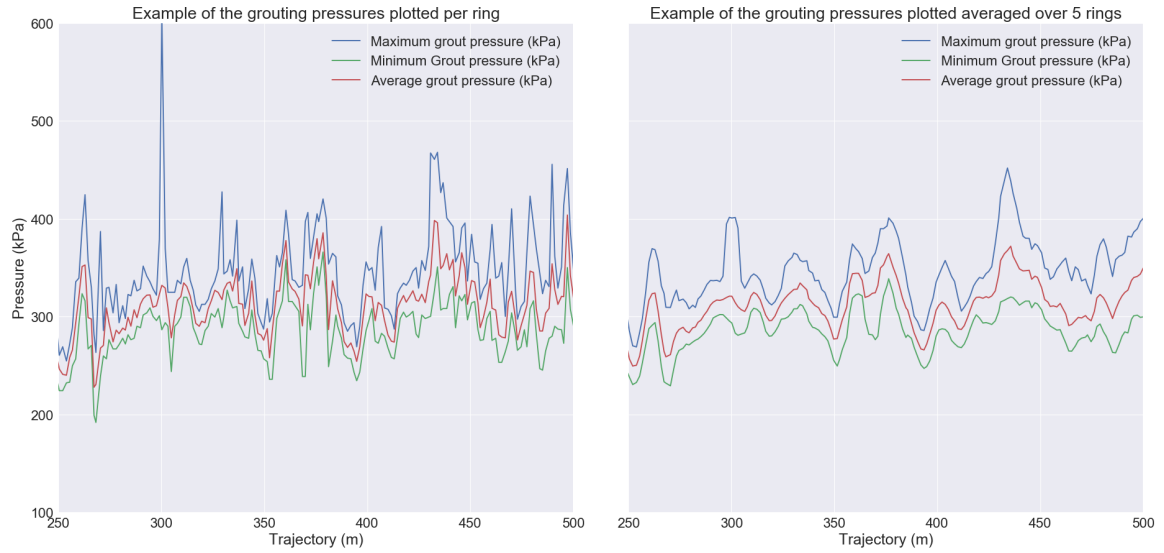


Figure 4.1: Example of a plot using the grout pressures per ring(left) and averaged over 5 rings(right).

4.1.3. Grout Volume

To analyse the injected grout volume, a comparable method is used. The left side of figure 4.2 shows the used grout volumes per ring. Again, the fluctuations in the graph are very large making it difficult to recognise trends. As detecting larger trends is more important than local fluctuations, the volumes are averaged over 5 rings (right side of figure 4.2).

Since the size of the tail void differs per project, it makes more sense to express the used grout volume relative to the size of the tail void rather than as an absolute number. Therefore, grouting volume will be represented as a percentage of the size of the tail void. In order to do so, the size of the tail void has to be calculated first. As seen in chapter 3, the tail of the TBM has a diameter of 6.870 m while the outer diameter of the lining is 6.500 m. The volume of the tail void over 1 meter of tunnel length can be found by taking the area of the tail of the TBM, subtracted by the area of the outside of the lining (equation 4.1). This results in a tail void volume of 5.83 m³/m. Now the used grout volume can be expressed relative to the size of the tail void.

$$V_{tv} = A_{tv} * l_r = (\pi * r_{st}^2 - \pi * r_l^2) = 3.89 m^3 \quad (4.1)$$

with:

r_l = Outer radius of the lining (m) = 3.250 m

r_{st} = Radius of the tail of the TBM shield (m) = 3.435 m

A_{tv} = Cross-sectional area of the tail void(m²)

V_{tv} = Volume of the tail void over the length of 1 ring (m³)

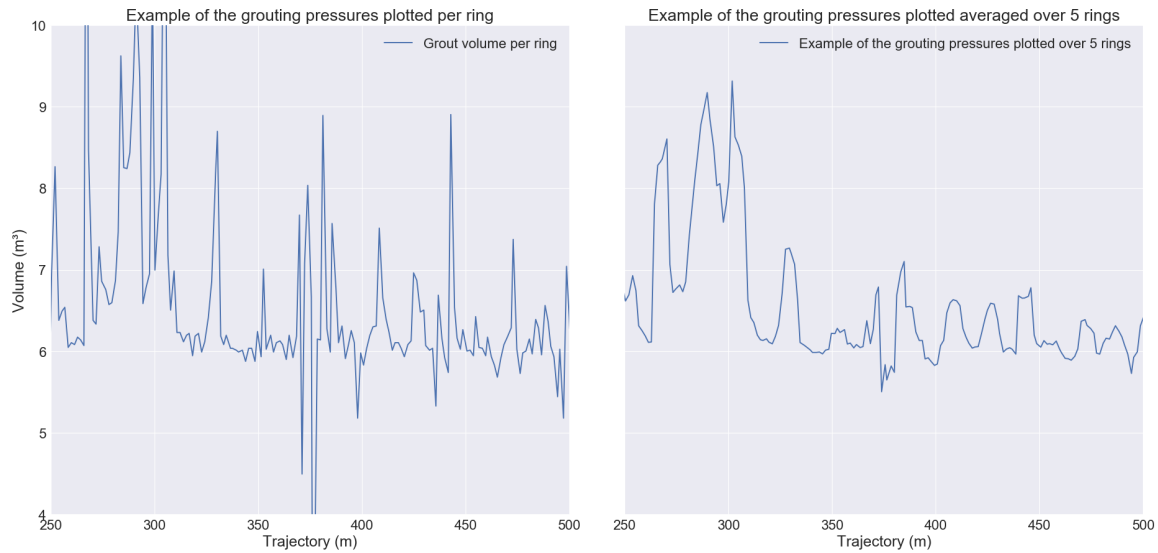


Figure 4.2: Example of a plot using the grout volumes per ring (left) and averaged over 5 rings (right).

4.2. RT1

The RT1 section is the most northern section of the boring trajectory. Consisting two tubes drilled from the Central station in the North to station Rokin about 1 km to the South, as explained in chapter 3.

4.2.1. Settlements

Figures 4.3 and 4.4 show the final settlements of the western and eastern trajectories of the RT1 section. For both trajectories 3 locations where the settlements change abruptly are indicated. The western trajectory starts with two sudden decreases in settlements (zone 1 and 2). In the end of this trajectory a sudden up and down movement in the settlements is selected. In the eastern trajectory (4.4) two dips in the settlements are selected as zone 1 and 2 and again in zone 3 an up and down movement of the settlements is selected.

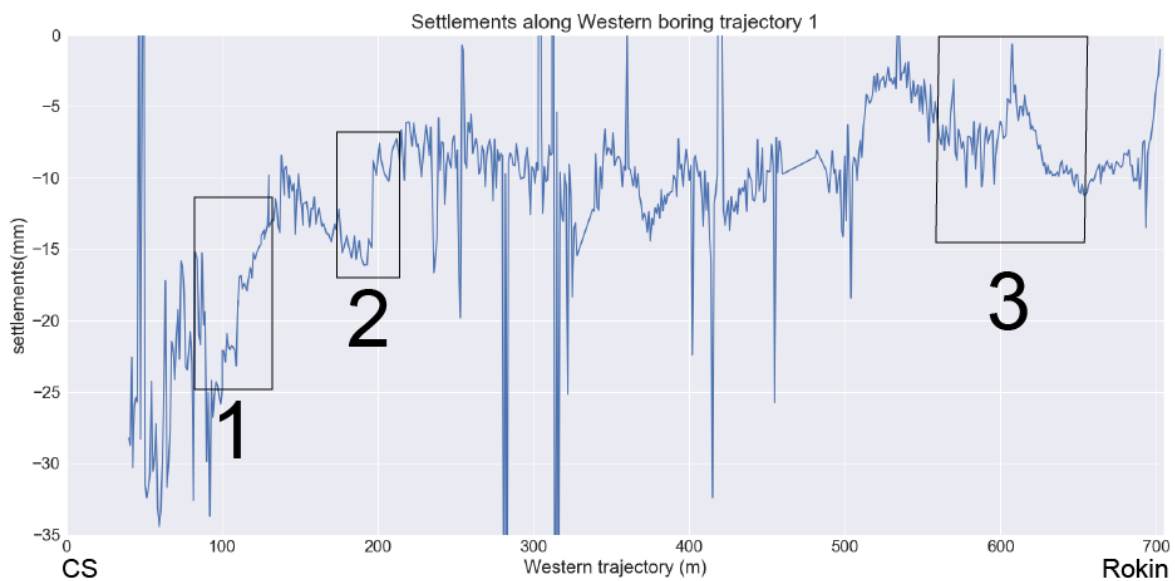


Figure 4.3: Settlement profile of the RT1 West trajectory divided in sections based on the settlements.

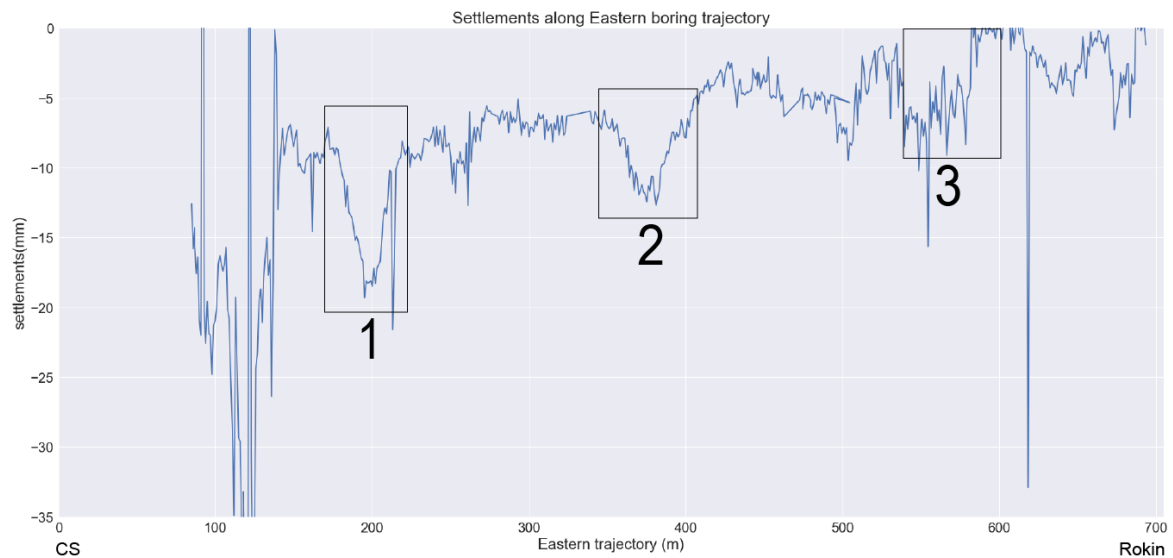


Figure 4.4: Settlement profile of the RT1 East trajectory divided in sections based on the settlements.

4.2.2. Grout pressure

Figure 4.5 shows the measured grout pressures during the boring of the RT1 West section. Zone 1, 2 and 3 show the locations of the zones selected in paragraph 4.2.1. For zone 1 the decrease of settlements coincides with a increase in the pressures. The settlements in zone 2 showed again an increase in the settlements, the pressures show a short peak on this location, but go down back to their level before the peak while the settlements do not increase again. For varying settlements in zone 3 the pressures stay quite constant.

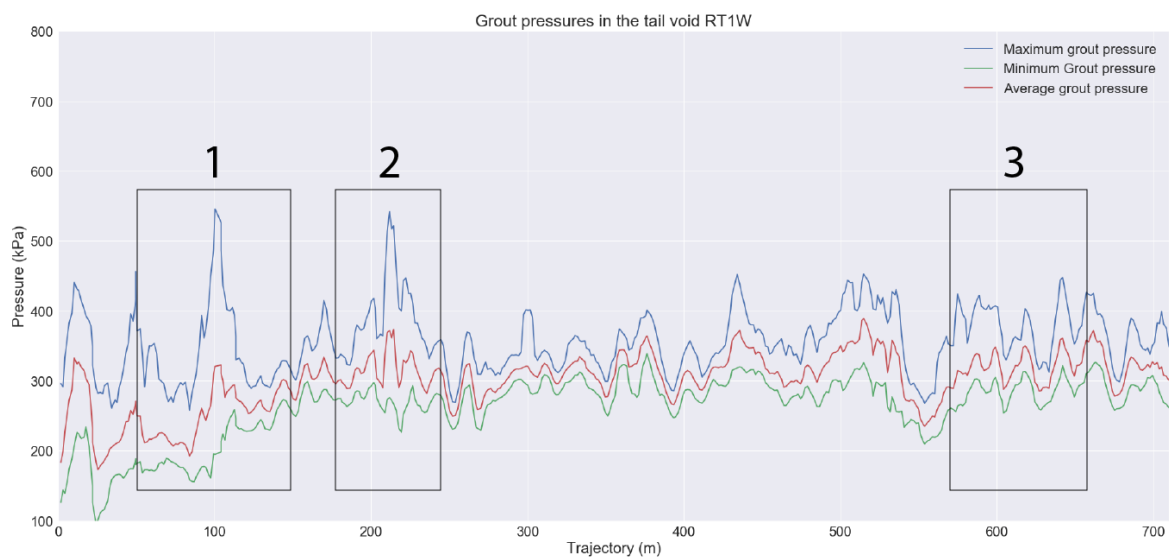


Figure 4.5: Measured grout pressures in the tail void of the RT1 West trajectory

The grouting pressures of the eastern tube of the RT1 section (figure 4.6) show an increase in the pressures in zone 1, the settlements however increase and decrease again not coinciding with the pressures. The pressures in zone 2 stay quite constant apart from one small peak, while the settlements at this location show a dip.

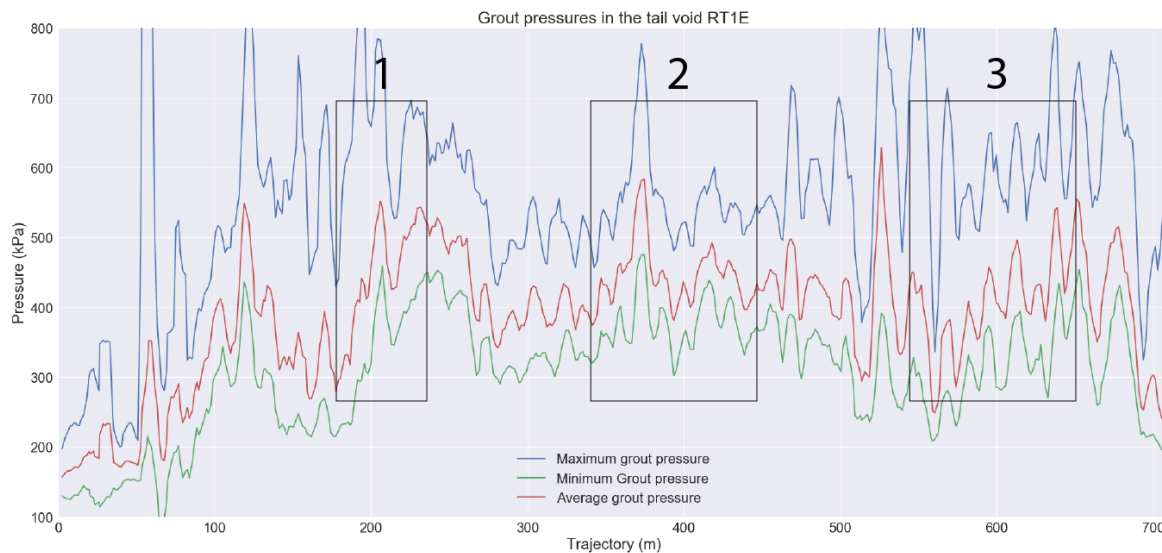


Figure 4.6: Measured grout pressures in the tail void of the RT1 East trajectory

4.2.3. Grout volume

Figure 4.7 shows the used grout volumes during the boring of the RT1 West section. In zone 1 the injected grout volumes drop dramatically, while the settlements decrease. Then, just before zone 2 the pressures drop underneath 100% of the tail void, the settlements also increase there. At 200m the grout volumes suddenly increase, at the same time the settlements decrease. In the third zone of the RT1W trajectory the injected grout volumes vary a bit, while the settlements go up and down.

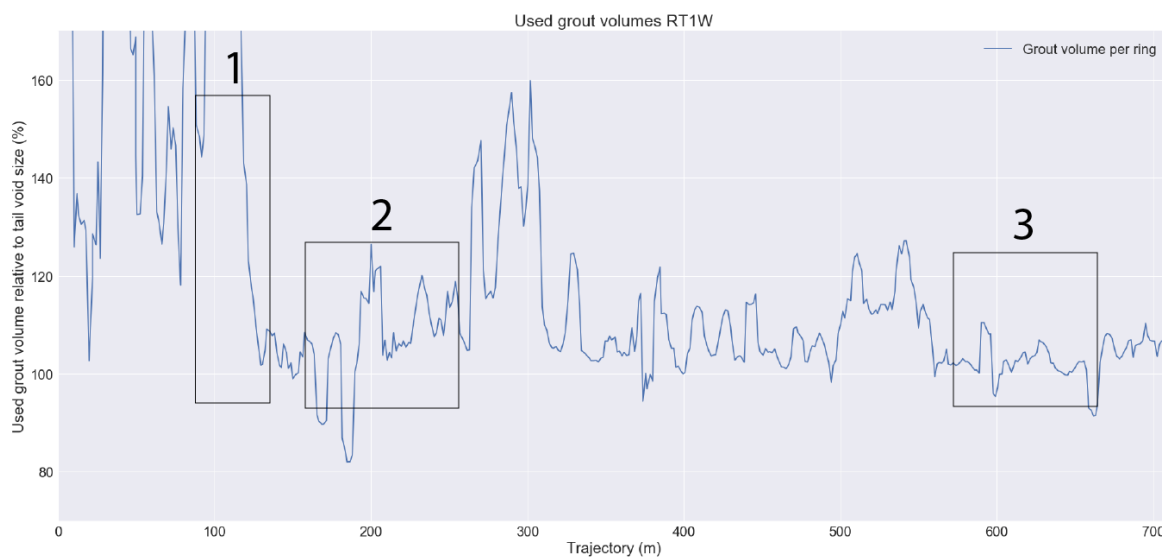


Figure 4.7: Used grout volumes during the boring of the RT1 West trajectory.

Figure 4.6 show the injected grout volumes of the RT1 East trajectory. In zone 1 the used grout volumes come back from a very high start and fall shortly under the 100% fill grade. At the same moment the settlements show a dip which is restored when the injected grout volumes increase again. In zone 2 the grout volume increases overall but is shortly underneath the 100%. The settlements show a dip in this zone but restore to a lower value after this dip. In zone 3 the grout volumes increase while the settlements almost totally disappear.

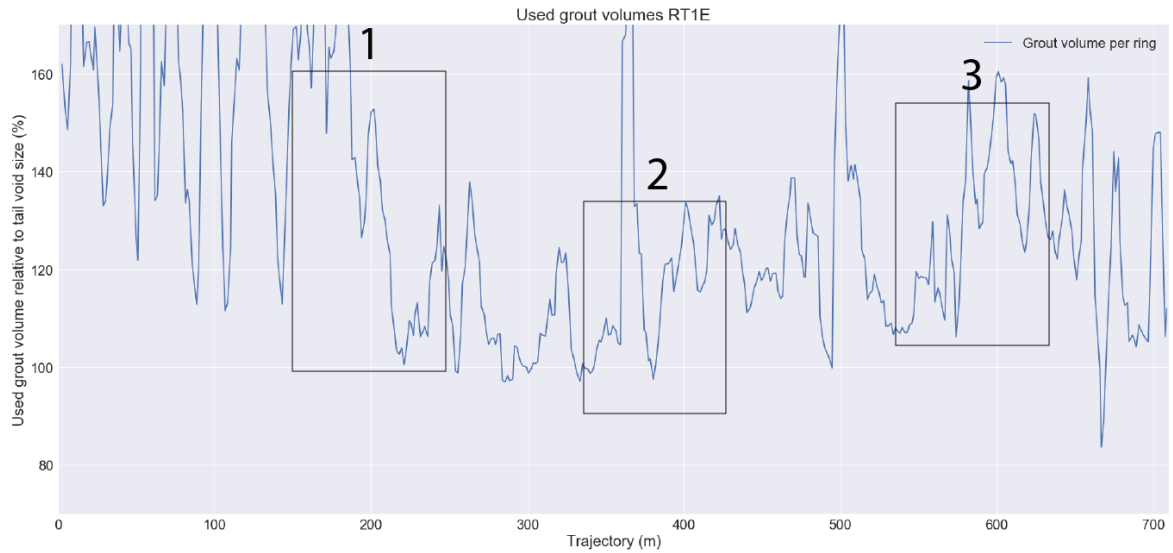


Figure 4.8: Used grout volumes during the boring of the RT1 East trajectory.

4.2.4. Subsurface

Figure 4.9 shows the lithology of the first trajectory. While the lithology stays quite constant over most of the zones. The first zone of the western trajectory (RT1W1) is located just after some very weak soils. This is a possible cause for the change in settlements.

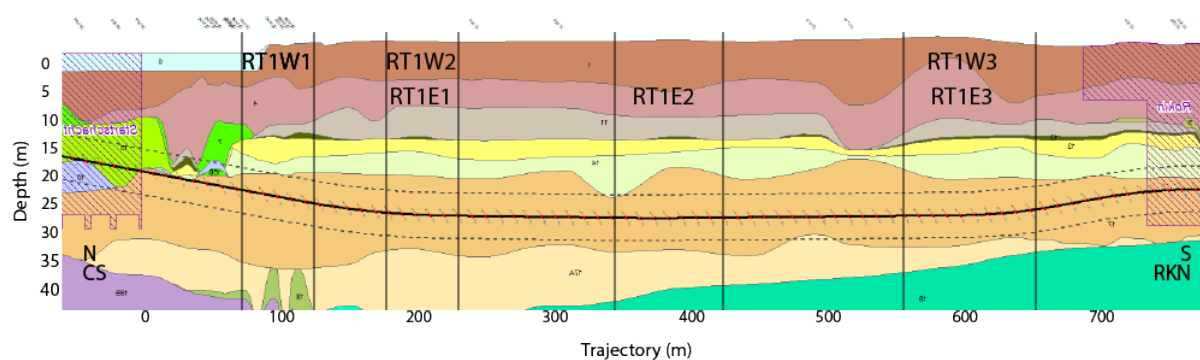


Figure 4.9: Geotechnical profile of tunnel section RT1 and zones of interest.

4.3. RT4

The RT4 section consists of the two most southern tubes of the North-South line, bored from South to North. Both start very shallow whereafter the western tunnel dives under the eastern (see Chapter 3).

4.3.1. Settlements

Figure 4.10 shows the settlements of the western trajectory of the RT4 tunnel. After a start with a large amount of settlements zone 1 shows that these settlements are decreasing. Hereafter, the settlements first slightly increase whereafter a dip occurs just like in zones RT1E1 and RT1E2. Between zones 2 and 3 the settlements shortly decrease all the way to 0 mm, this location is ignored as a bridge which is founded on deeper layers is located and this does not show the actual induced settlements. In zone 3 the settlements show a decrease.

The RT4 East section is treated a little different than the others. Later research showed that the settlement measurements of this zone showed that it contained quite a lot of noise. This, combined with the small settlements, causing the noise to look even bigger in a normalised analysis, and that the TBM data of the beginning of the trajectory is not available lead to the decision pick 3 locations and analyse these. One could argue to leave the trajectory out, but since this it is the most shallow tunnel there is decided to leave it in. The locations are shown in figure 4.11.

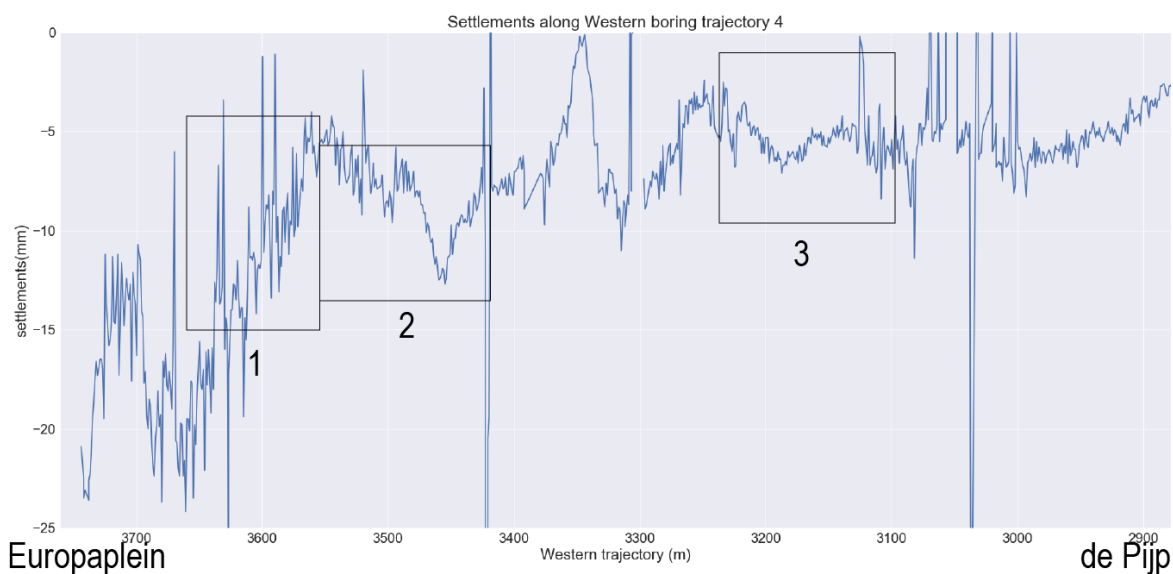


Figure 4.10: Settlement profile of the RT4 West trajectory divided in sections based on the settlements.

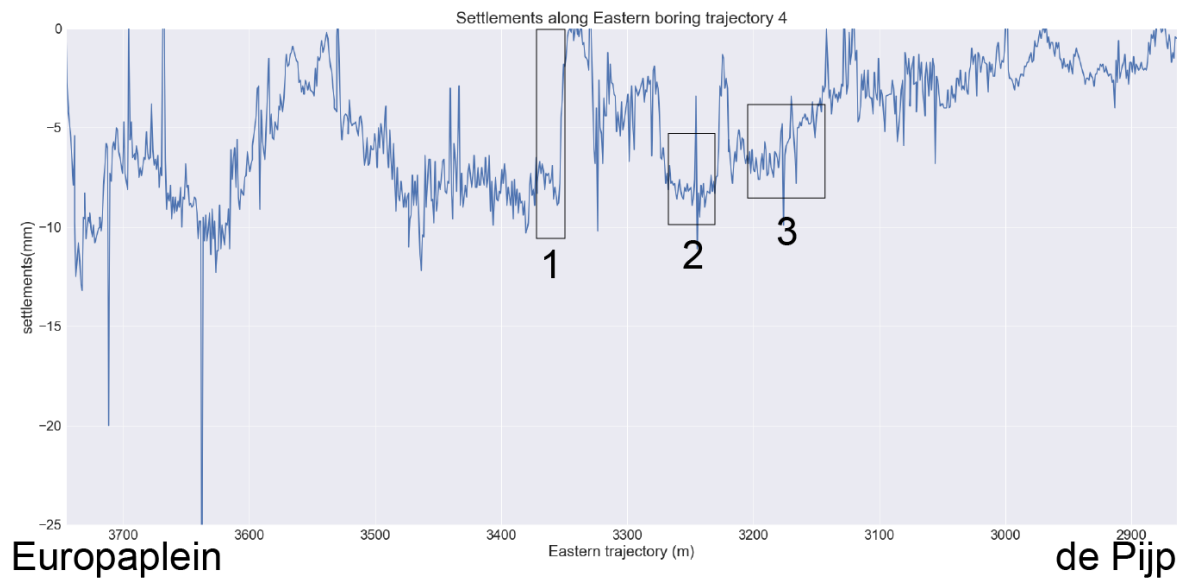


Figure 4.11: Settlement profile of the RT4 East trajectory divided in sections based on the settlements.

4.3.2. Grout pressure

Figure 4.12 shows the grout pressures of the RT4 West trajectory. The first and second zone show quite a constant pressure. While the settlements in zone 1 decrease and in zone 2 a dip in the settlements occurs. In zone 3 the pressures are a lot higher than before. During zone 3 the pressures decrease, the settlements in this zone slightly increase.

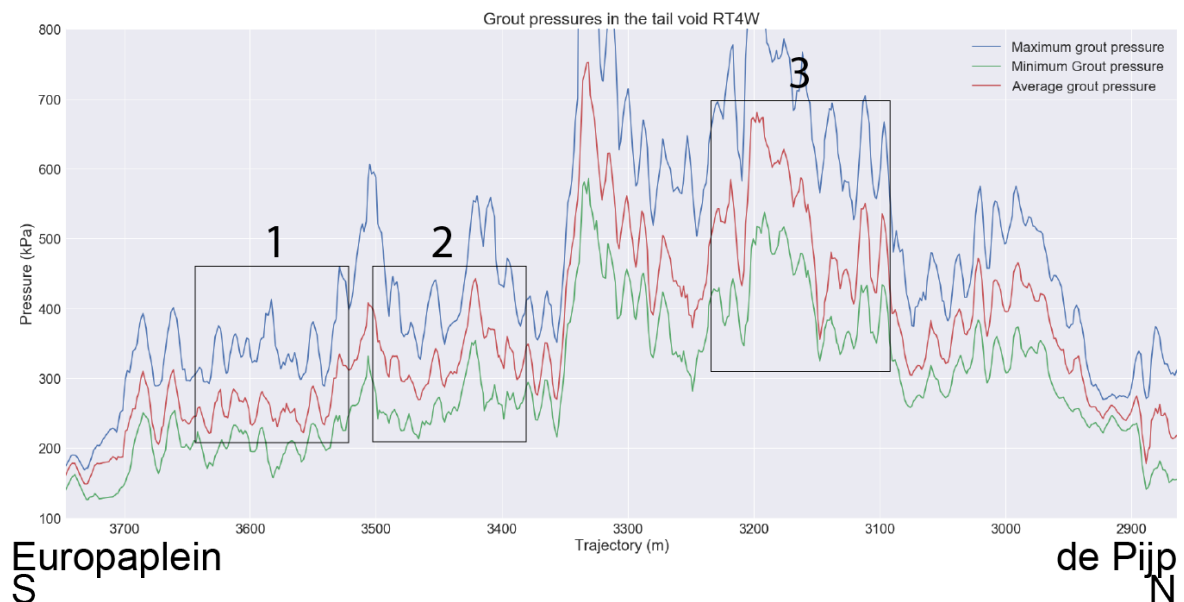


Figure 4.12: Measured grout pressures in the tail void of the RT4 West trajectory

Figure 4.13 shows the grout pressures of the RT4 East trajectory. As the zones of RT4 East are compared with each other instead of within the zone the grout pressures are also compared with each other. The grout pressures of zone 2 are slightly higher than those in zone 1. In zone 3 the grout pressures further increased. The settlements of zone 1 and 2 are equal while the settlements in zone 3 are slightly smaller.

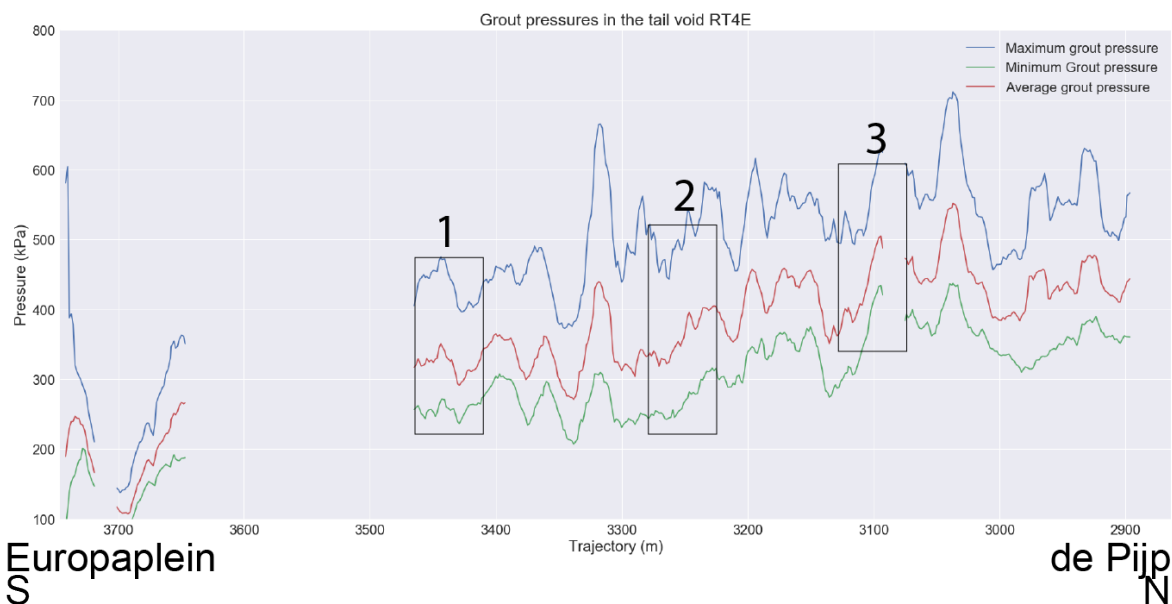


Figure 4.13: Measured grout pressures in the tail void of the RT4 East trajectory(gaps are due to missing data).

4.3.3. Grout volume

Figure 4.7 shows the injected grout volumes during the boring of the RT4 West trajectory. The first zone shows a slightly increasing grout volume coinciding with the decrease in settlements. The second zone shows a decrease in the injected grout volumes the volumes even dipped below 100% shortly. The settlements show a similar pattern. In the third zone the grout volumes stayed quite constant, while the settlements slightly decrease. Figure 4.15 shows the injected volumes of the RT4E trajectory. All three locations show similar injected grout volumes.

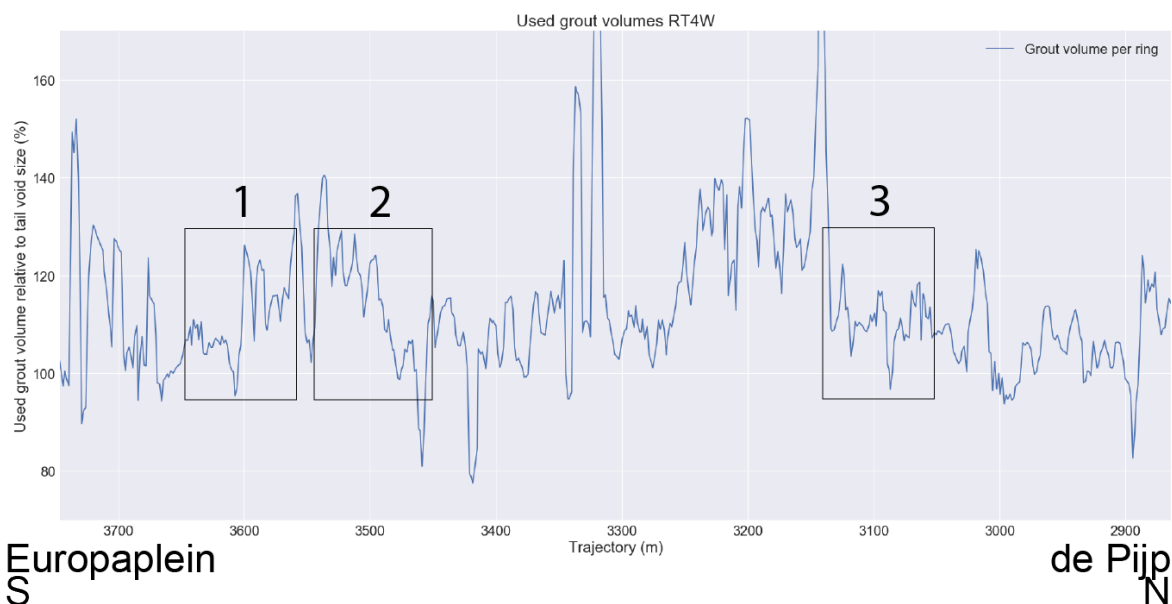


Figure 4.14: Used grout volumes during the boring of the RT4 West trajectory.

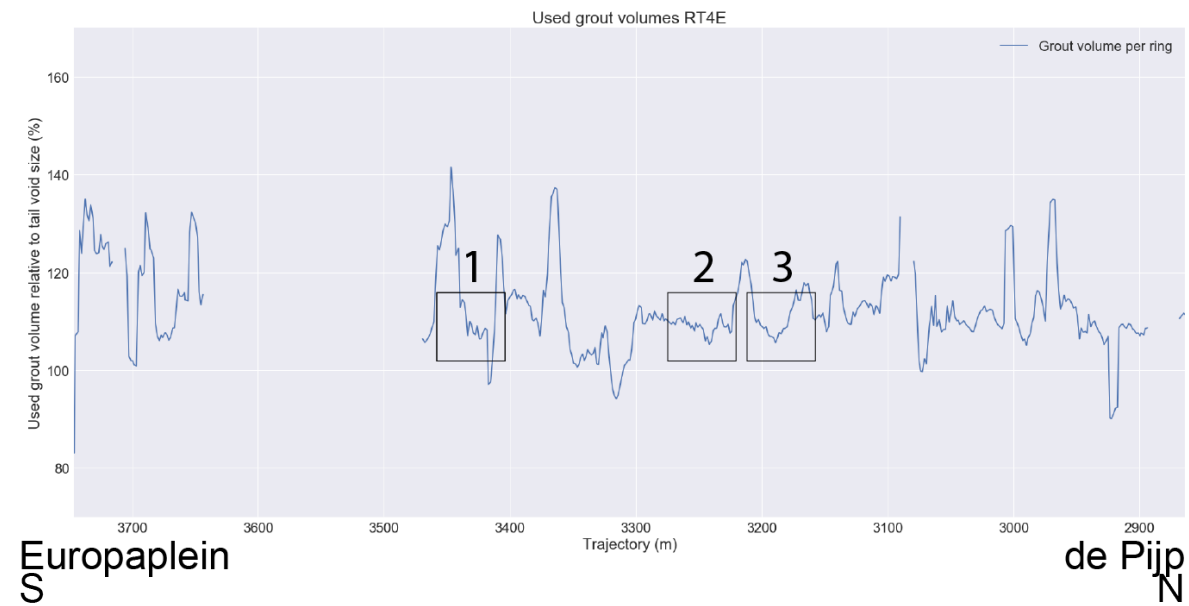


Figure 4.15: Used grout volumes during the boring of the RT4 East trajectory (gaps are due to missing data).

4.3.4. Subsurface

The subsurface of the RT4 section in figure 4.16 shows that both of the tunnels start very shallow and directly go down deeper, crossing multiple soil layers. The western tube stays relatively shallow, while the eastern tube dive under the western tube to almost 30 metres. At 3300m a channel is passed. Right above the tunnels a bridge is situated. To protect the foundations of the bridge both grouting pressures and front pressures are kept as low as possible before passing this bridge. The bridge also influences the settlement measurements as the surface of the bridge is measured while the bridge is founded in a deeper sand layer.

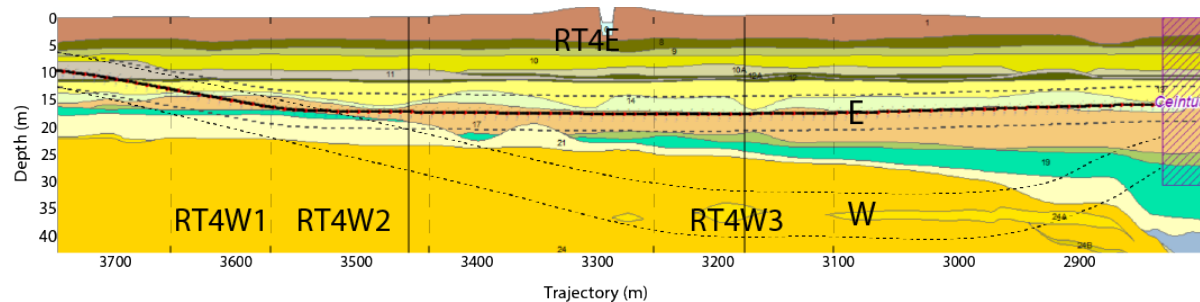


Figure 4.16: Geo-technical profile of tunnel section RT4 and points of interest.

4.4. Discussion

In this chapter the changes in settlements are compared with the grouting behaviour of the TBM. A decrease in settlements coincided with an increase in injected grout volume multiple times, with the grout pressures no such relation was found. Figure 4.17 shows the settlements of the locations selected in chapter 4, in order to relate the total settlements with the injected grout volumes and pressures. The wide spread of data points in this scatter plot illustrates that no direct relation can be found between the grouting behaviour and the total settlements.

It is remarkable that the injected seem to be able to change the settlements but do not relate with the total settlements. However, this can be explained by the fact that much more variables influence the total settlements. As the grout volume can decrease the settlements induced by the tail void it can not influence

these other parameters. Therefore, the settlements induced by the other components of the TBM or the change in settlements caused by the change in lithology probably overshadow the effect of the grout volume. In chapter 5 the settlements of the tail void will be isolated in order to assess the effect of the grouting on the tail void induced settlements.

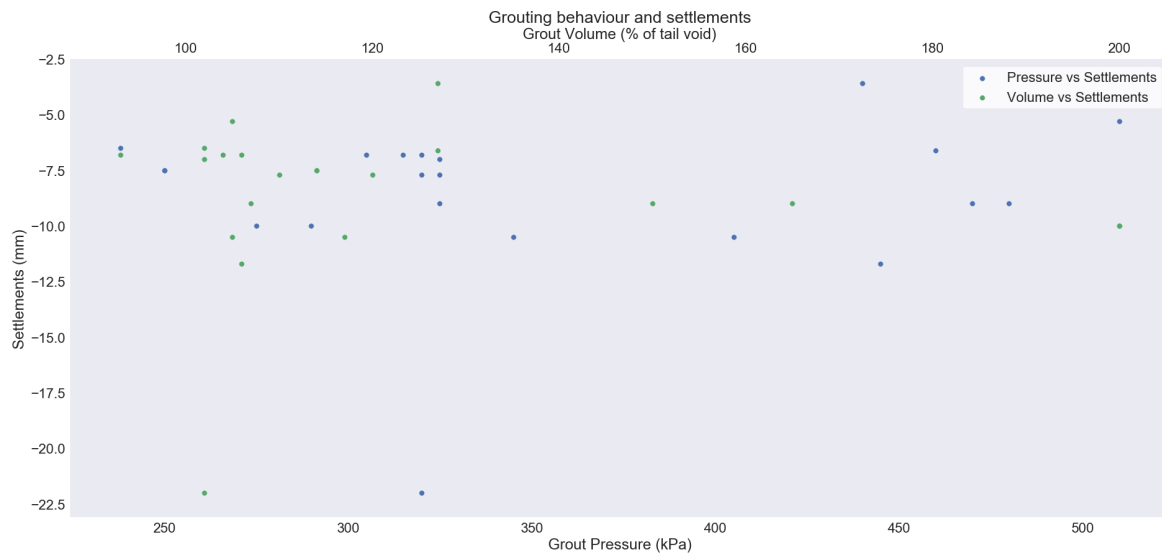


Figure 4.17: Scatter plot of the grout volumes injected in the tail void (top x axis) and the grout pressures in the tail void (bottom x axis) against the settlements.

Development of the settlements during the TBM passage

In chapter 4, the locations with sudden changes in settlements and grouting behaviour were indicated and checked for possible geological causes. In this chapter, these locations are further assessed to indicate which component of the TBM could be causing the sudden change in settlements. A settlement development curve is introduced which shows the settlements at one point of measurement as a function of the distance between the front of the TBM and this point of measurement. The settlement development curve thus shows which component of the TBM was underneath the point of measurement when the settlements took place. This is some indication for which component of the TBM is responsible for these settlements. In reality however, the induced settlements do not only appear straight above their source, but also further away from this point as seen in paragraph 2.2. To create a sense of the size of these influence zones the distance between the first appearing settlements and the front of the TBM is checked, with the assumption that the first appearing settlements are induced by the front of the TBM.

When the zones of influence are known, this can be used to assign the share of each component of the TBM has in the total settlements. The zone of influence can be combined with the knowledge from the settlement development curve on which component of the TBM was underneath the point of measurement during a certain part of the settlements. This provides an indication on which component of the TBM is causing which part of the settlements.

5.1. Zone of influence

Settlements induced by the front of the TBM are the first ones to be measured. Thus, the zone of influence can be derived from the distance between the point of measurement and the location of the front of the TBM at the time when the first settlements are measured. Since the other components of the TBM are in roughly the same lithology, the zones of influence of all components of the TBM are expected to be of the same size. This assumption was applied in all further analyses.

The location of the first measured settlements is derived from the settlement development curve in figure 5.1. A line is drawn through the first appearing settlements. At the point this line crosses the 0 settlement line (the x-axis at the top of the graph), is chosen as the point of first settlements. This is done for three parts of the tunnel with constant depth. The results of this are shown in figure 5.2. It can be seen that a deeper tunnel creates a wider zone of influence. Therefore, it is more difficult to assign parts of the total settlements back to the separate components of the TBM. Also, the spread in the sizes of the zones of influences increases. This is probably because more soil layers are passed, adding a bigger uncertainty.

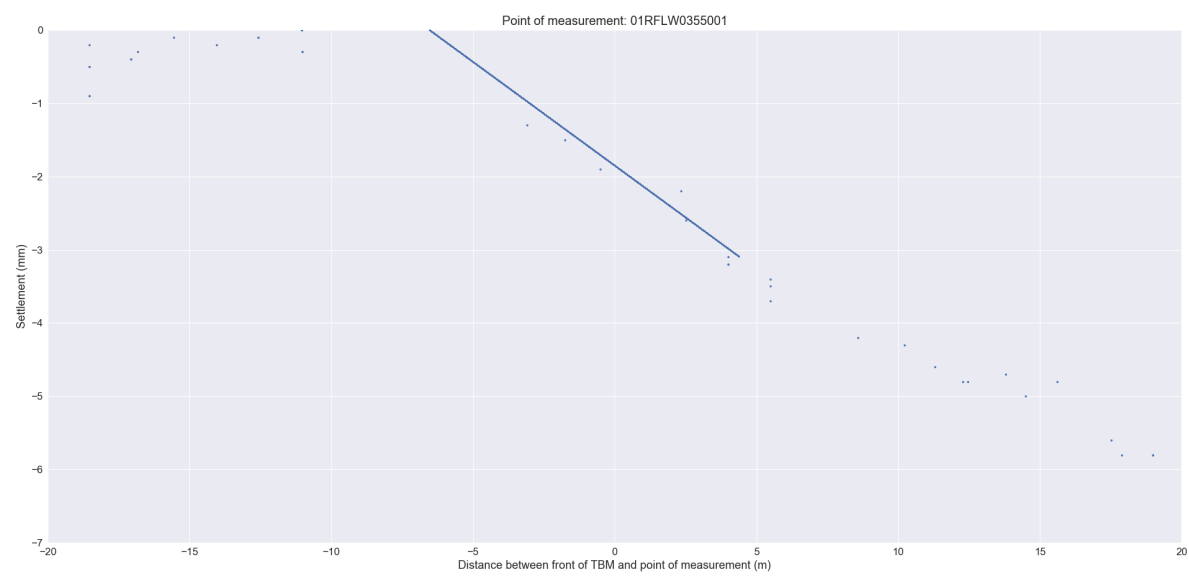


Figure 5.1: Example of determination of the point of inflection.

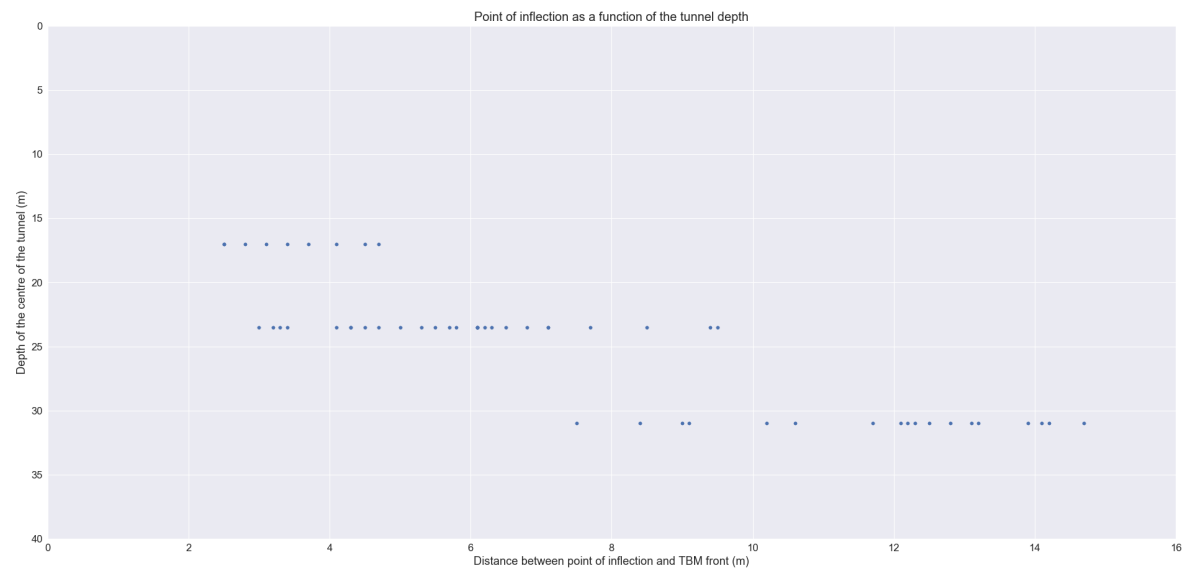


Figure 5.2: Graphically image of inflection points at different tunnel depths

5.2. The normalised settlement development curve

The goal of the settlement development curve is to identify whether a particular component of the TBM is responsible for a change in settlements and if so, which component this is. When comparing different locations, like before and after the 200 meter mark of RT1 West some problems occur. Figure 5.3 shows that the relatively large difference in total settlements makes it difficult to compare the phases of the settlements. To overcome these problems, a normalised settlement development curve is introduced. The settlement development curve is divided by its maximum settlement, making all curves run from 0 to 1. If one location causes more settlements than usual, this will now be visible in the normalised settlement curve. The normalised version of figure 5.3 can be found in figures 5.4 and 5.5(zoomed in). The overlapping of the curves illustrate that the soil at both measurement points settles at the same rate with respect to the total settlements. However, at a distance of around 15m, the settlements of measurement point 01RFLW0203001 stabilise, while the settlements at measurement point 01RFLW0187001 keep increasing.

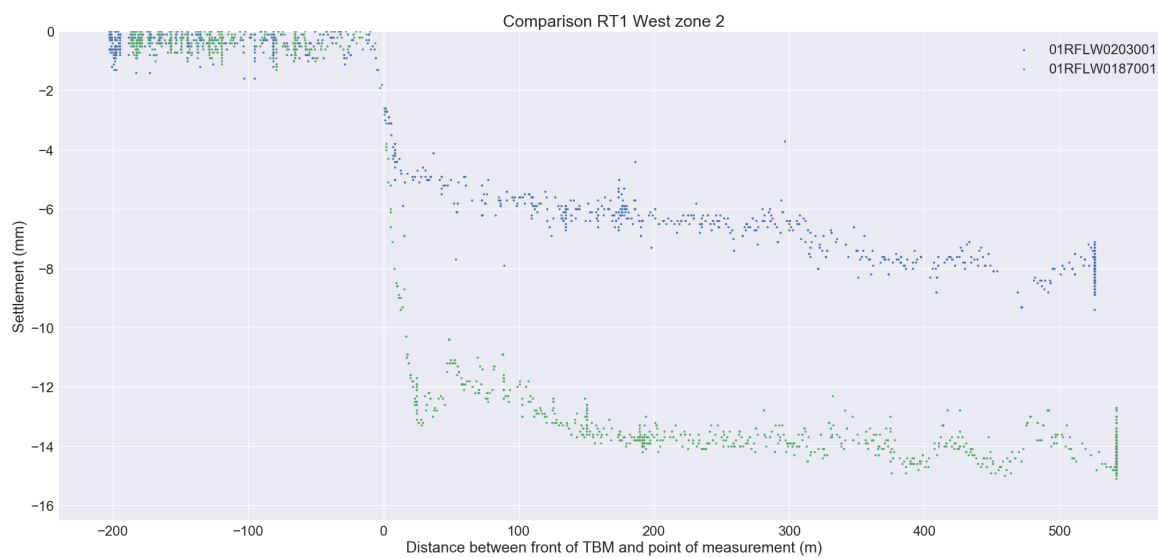


Figure 5.3: Settlement development curve comparison RT1 West zone 2.

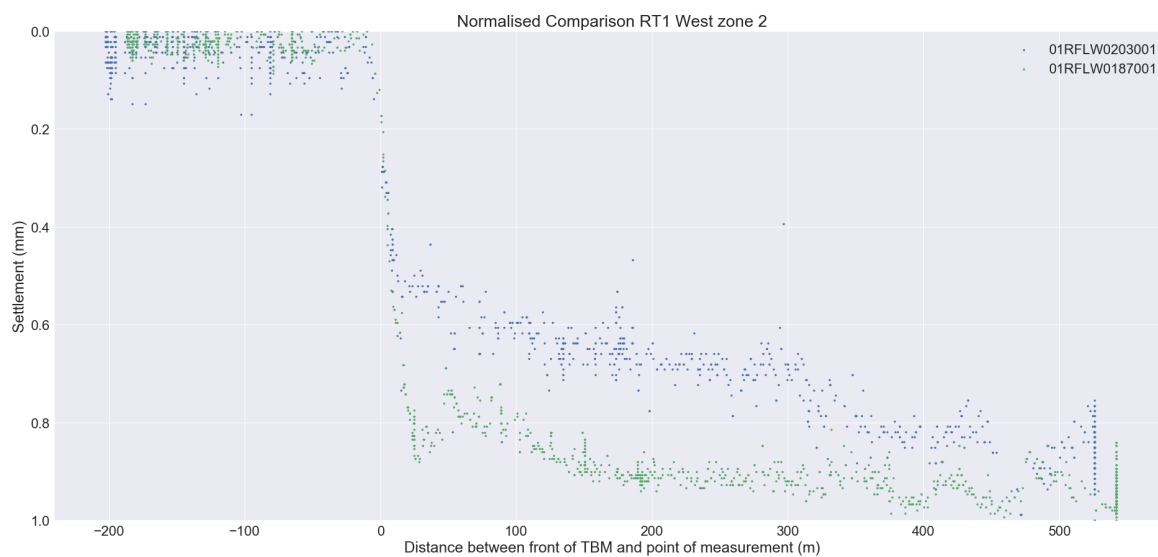


Figure 5.4: Normalised settlement development curve comparison RT1 West zone 2.

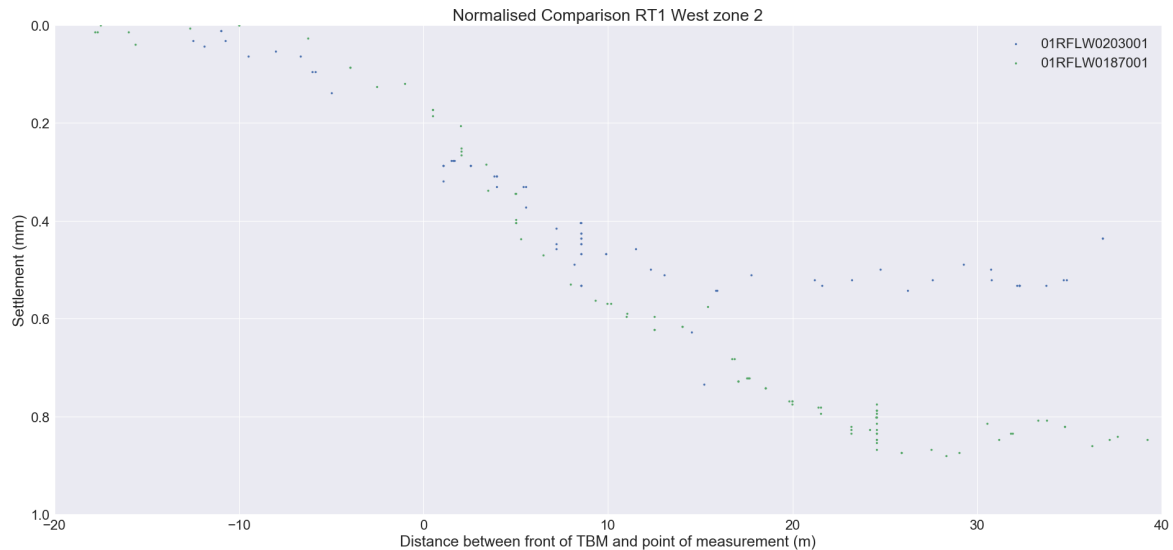


Figure 5.5: Normalised settlement development curve comparison RT1 West zone 2.

5.3. Average settlement curve

The settlement development curves above only use one location of measurement. In chapter 4 it was shown that the settlements stay quite constant over a period, after which changes often happen rather quickly. This can be used to make the data more reliable and to increase the amount of measurements at the moment the TBM passes. To do so an average settlement development curve is introduced. This averaging can be done in several ways. The most easy way is to create a rolling window over the indices of the total data set. However, physically this means that you average over a certain amount of measurements independent of the forward movement of the TBM. This means that the speed of the TBM would influence the window size. Therefore, the window size is based size on the distance between the front of the TBM and the point of measurement. In figure 5.6, the results of six different measurement points are visualised together. These are all located in the RT1 West trajectory within a range of 10 meters of each other. The graphs shows although the measurements vary slightly, none of the measurement points differs much from the others, opposed to occurrence in figure 5.3. The suitability of different window sizes are compared. Increasing the window size oppresses the noise in the measurement, but big outliers will influence a bigger area when a bigger window is used. Decreasing the window size will show more noise, but outliers will influence a smaller area and can therefore be spotted easier. This can be seen in figure 5.7, when looking at the area around 25 meter. The rolling averages with window sizes of 5 and 10 metres show a less high but quite broad peak, which insinuates a heave. The 1 meter rolling average shows a high but narrow peak, easily recognisable as an outlier. Another point where the averages differ a lot is during the passage of the TBM underneath the point of measurement, around 0 meter. Here it looks like the bigger windows 'cut the corner' while the small 1 meter window stays in the point cloud. Therefore it is decided to use the 1 meter window.

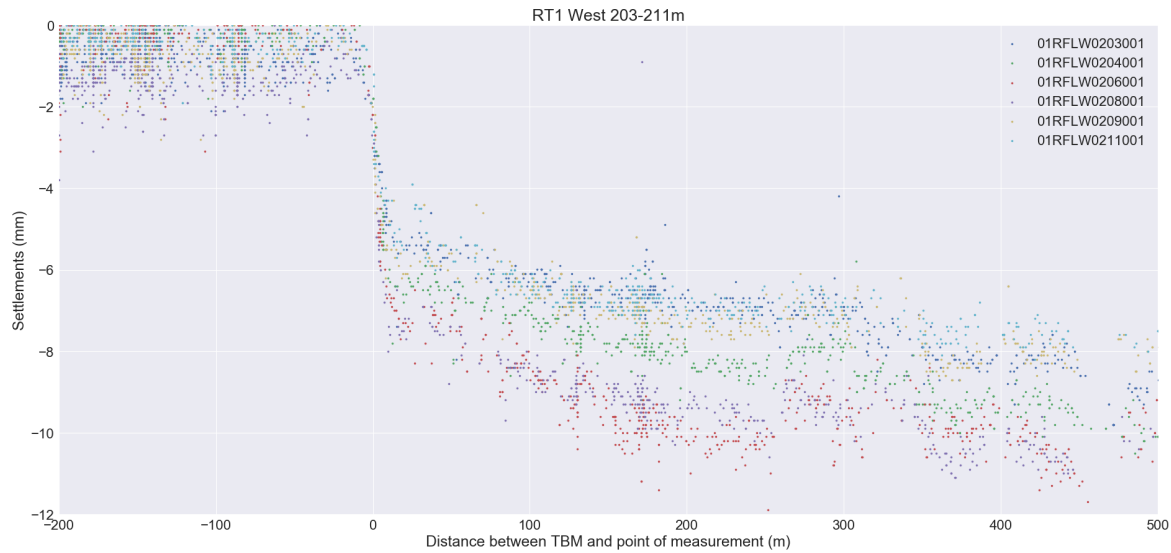


Figure 5.6: Measurements of RT1 West between 203m and 211m.



Figure 5.7: Measurements of RT1 West between 203m and 211m with the influence of the size of the window.

5.4. Settlement development at zones of interest

In this paragraph, the zones of interest found in chapter 4 will be further assessed. To indicate which component of the TBM is responsible for the settlements, the average settlement curves explained in paragraph 5.3 will be used. Although these give a certain indication of which component of the TBM is responsible for the settlements, they should be used with care. As seen in paragraph 5.1, the zones of influence of the different components of the TBM overlap, making it difficult to distinct them from each other.

5.4.1. RT1 West zone 1

To find a cause of the big change in settlements in zone 1 of the RT1 Western trajectory, the settlement development before (101-109m) and after (112-117m) the big change in settlements are compared. To do so, the average settlement curves are compared in figure 5.8. In this figure, it can be seen that both average settlement curves start settling at the same moment. However, the 101-109m curve reaches a larger total set-

tlement. Following this graph it is difficult to say whether one curve performs better than the other in a certain region. Therefore, the normalised settlement curve is shown in figure 5.9. This shows that the curves overlap each other almost perfectly. This implies that the TBM behaviour was not changing significantly during the sudden change in settlements.

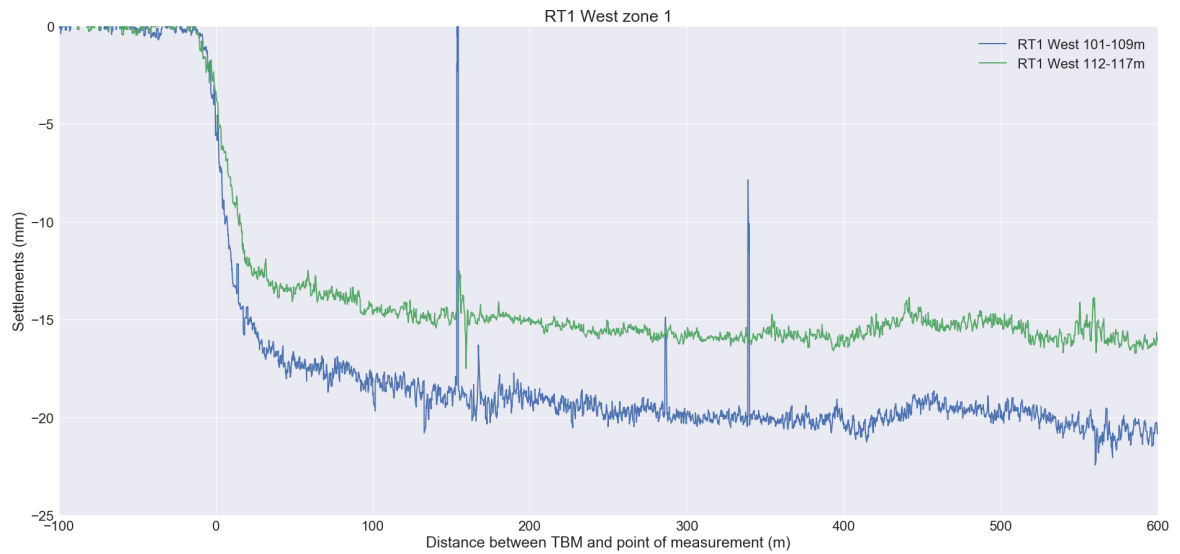


Figure 5.8: Comparison of the average settlement development curves of RT1 West zone 1.

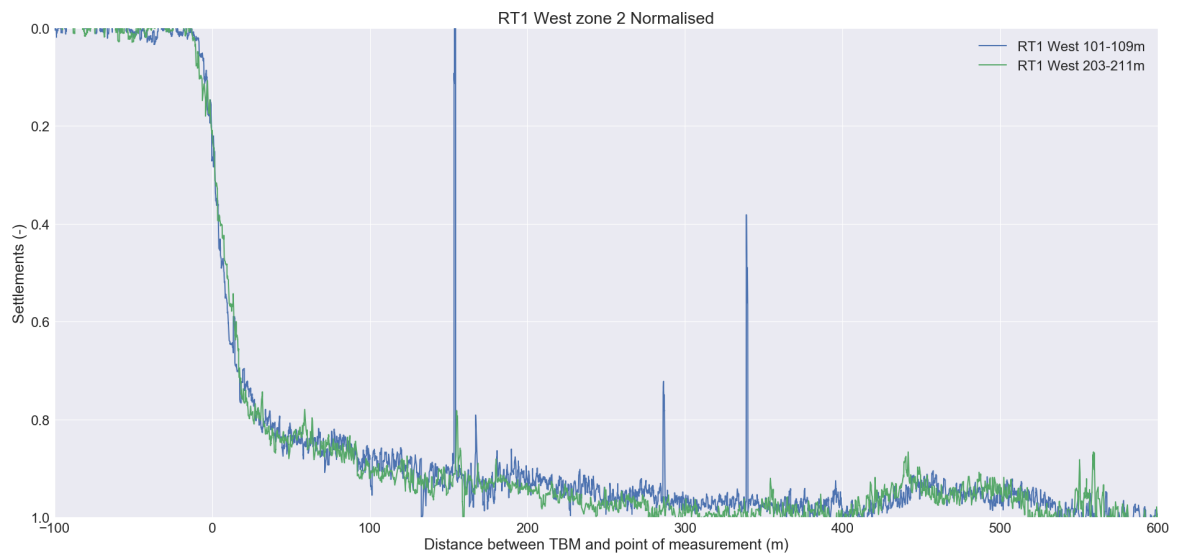


Figure 5.9: Comparison of the normalised average settlement development curves of RT1 West zone 1.

5.4.2. RT1 West zone 2

The RT1 West zone 2 is used as an example and the construction of the average curve can be seen in figures 5.6 and 5.7. Now the same is done for the area just before the change in total settlements. Comparing these two graphs in figures 5.10 and 5.11 while they have different final -settlements both graphs stay on about the same path until the front of the TBM passed the points of measurement by 4 meters. Thereafter, the 187-195m zone settles another 7 millimetres while the 203-211m stabilises at around 7 mm. When these graphs get normalised in figure 5.12 it can be seen that the graphs overlap for the biggest part of the figure except for the region between 11 and 50 meters. The reason the graphs come together and do not go down together parallel looks like a heave in the 187-195m graph. However when looking at the zoomed in graph, figure 5.11, it can be seen that this is only just over 1 mm and the same behaviour can be seen at 300-400m in figure 5.10. Therefore the 30m mark, where the 187-195m graph seems to stabilise is considered as the end of the region where the difference is made.

Linking this 11 to 30m after the front of the TBM passed the point of measurement to a component of the TBM is difficult as seen in paragraph 5.1. In figures 5.10-5.12 it can be seen that the inflection point lies around 7 meter, this 7 meter can be taken as the zone of influence of the TBM components forward as well as backwards

Altogether the difference in total settlements seem to be created in the region It looks like this is the region where the difference is made. An attempt to link this to a region of the TBM can be made using the inflection point as zone of influence. For these graphs this is approximately 7 meters. Combining this 7 meters with the above found 11-30 meters it can be seen that the TBM components responsible for these are lay between 4 and 37 meter behind the front of the TBM, these are the last 3 meters of the shield and the tail void of the TBM. Because the tail of the TBM is located at 7 meters behind the front of the TBM its influence stops at 14 meters behind the TBM, so only 3 meters in above constructed 11-30 meters where the difference is made. Although this still has to be confirmed by the data from the grouting process(chapter 4) it looks like the tail void is responsible for the change in settlements.

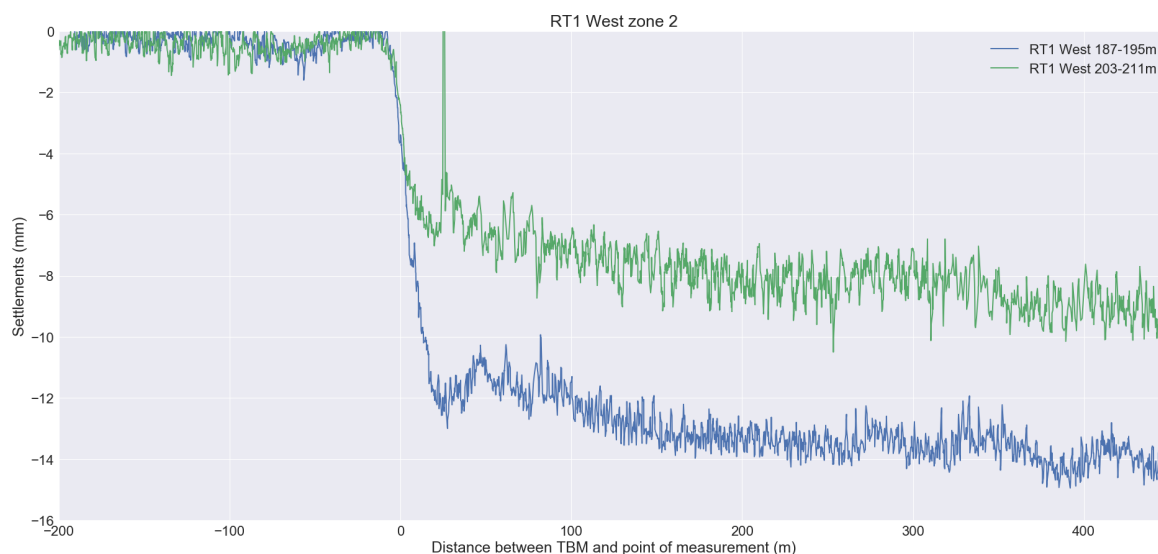


Figure 5.10: Comparison between the regions just before and after zone 2 in RT1West

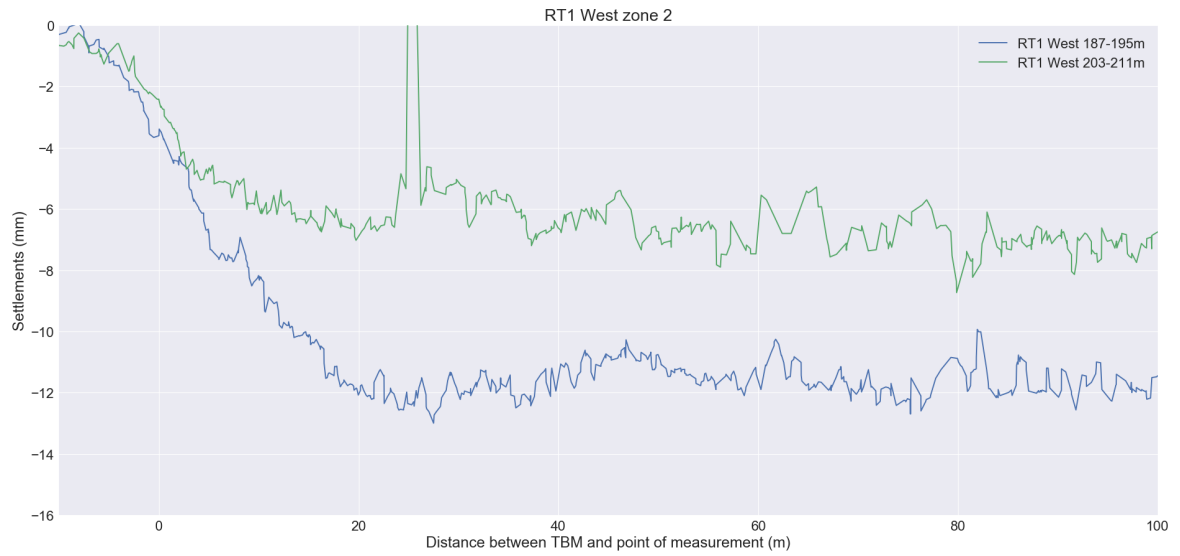


Figure 5.11: Zoomed comparison between the regions just before and after zone 2 in RT1West.

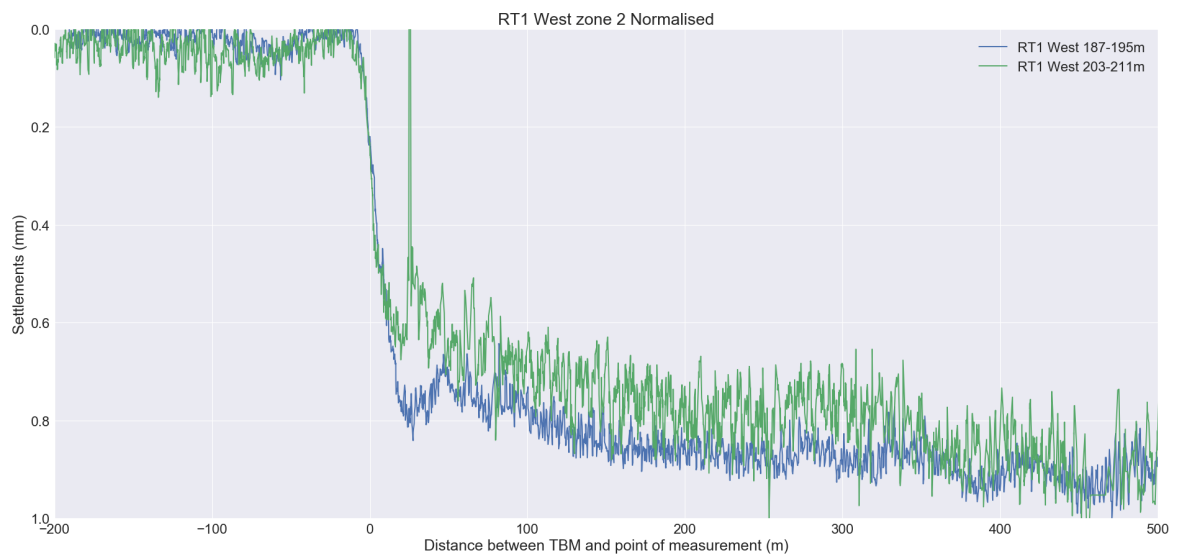


Figure 5.12: Normalised comparison between the regions just before and after zone 2 in RT1West.

5.4.3. RT1 West zone 3

RT1 West zone 3 is a zone with a lot of fluctuations in the total settlements. An attempt is made to make average settlement curves before and after each of these movements. However, due to the very small settlements the noise in data was too big of a part in the actual data to be able to construct the average settlement curves. Therefore for this zone the average settlement curves are created only for the section 580-585m and the section 650-656m. The construction of these curves can be found in figures ??-??. These average settlement curves are combined in figure 5.13. It can be seen that these are two completely different curves. The 580-585m starts settling very early, the 650-656m curve does that much later however drops down all the way to 9 mm and stops settling at around 12 meters after the front of the TBM has passed, while the 580-585 keeps settling until the 40m after the front of the TBM has passed. This can again be seen in the normalised curves in figure 5.14.

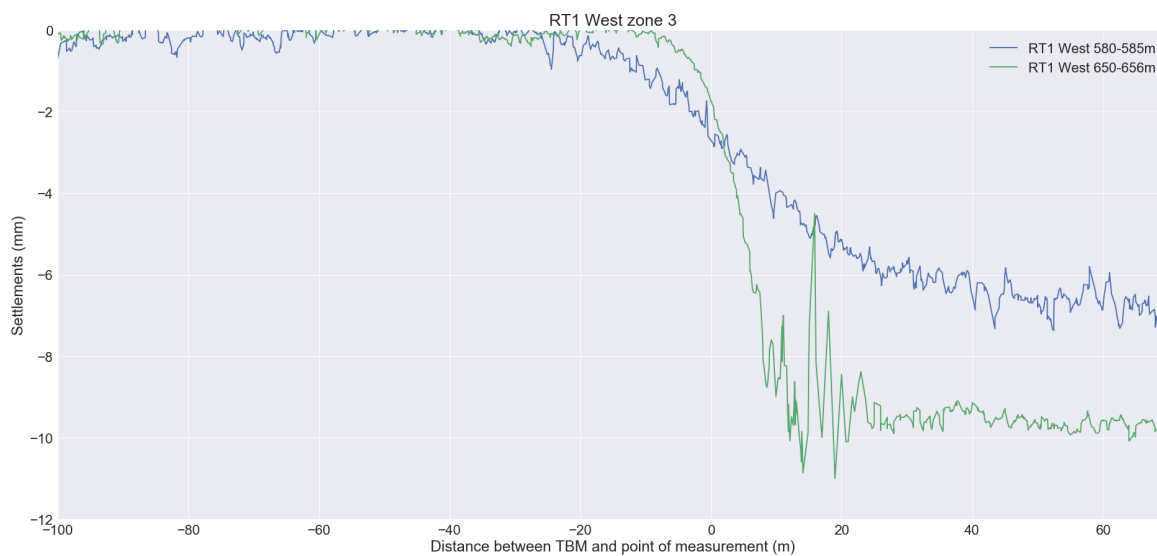


Figure 5.13: Comparison of the average settlement development curves of RT1 West zone 3.

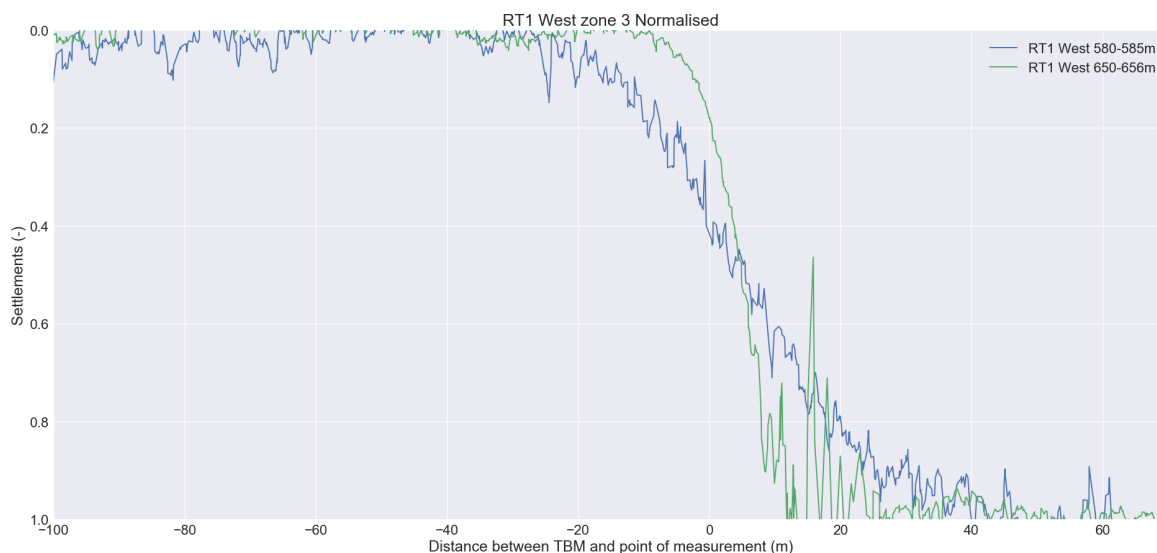


Figure 5.14: Comparison of the normalised average settlement development curves of RT1 West zone 3.

5.4.4. RT1 East zone 1

In Figure 5.15 the average settlement development curves of three locations around zone 1 of the RT1 East section. It can be seen that the area of 197-203 m underwent almost 10 mm more settlements than the other two sections. While it looks like the 173-180m and 212-219m sections had a quite similar settlement development profile. Comparing the normalised settlement development curves in figure 5.16 it can be seen that all of the three curves have undergone quite similar settlement development patterns. This indicates that the change in settlements is not caused by one particular component of the TBM.

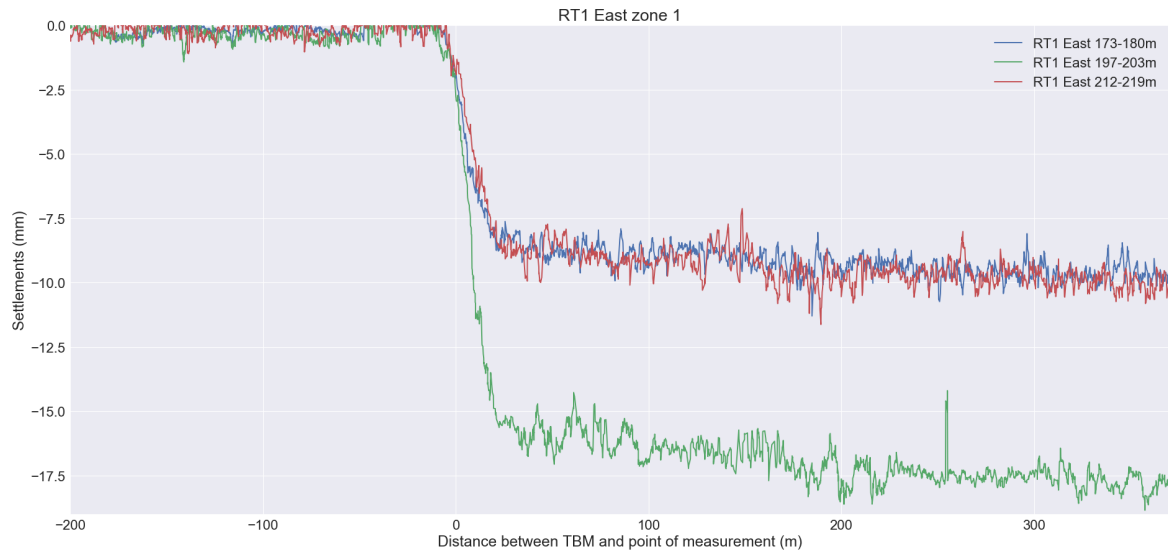


Figure 5.15: Comparison of the average settlement development curves of RT1 East zone 1.

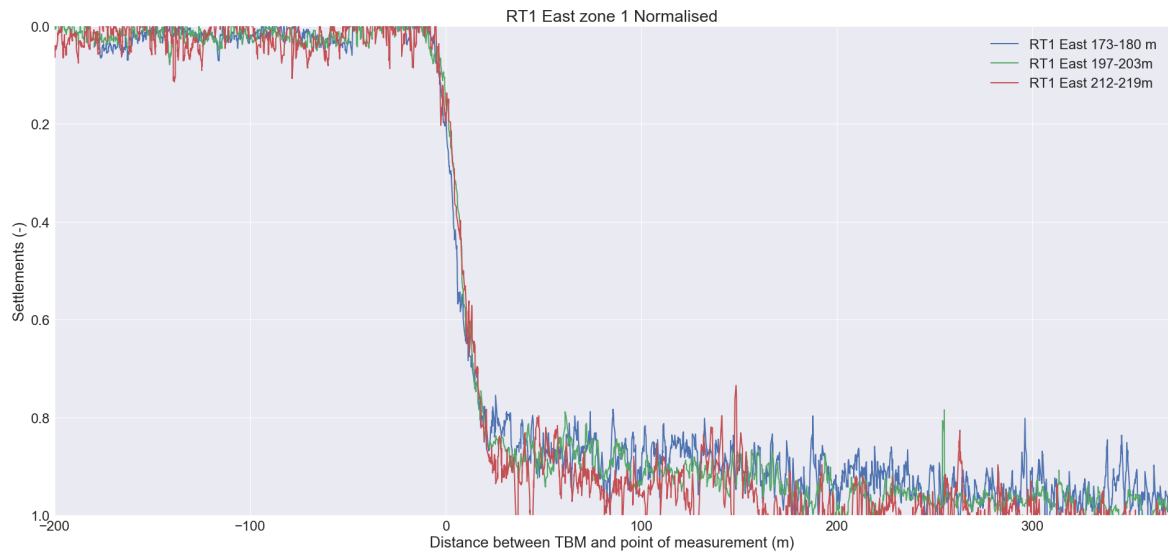


Figure 5.16: Comparison of the normalised average settlement development curves of RT1 East zone 1.

5.4.5. RT1 East zone 2

For RT1 East zone 2 three different locations are compared. Before, during and after the dip in settlements. In figure 5.17 the three different settlement development curves of zone 2 are shown. In the normalised version of the curve, in figure 5.18 it looks like the three curves are comparable. When looking closer however, it can be seen that the settlements of the 422-426m line reach their maximum settlements much earlier than the other two, indicating better performance of tail of the TBM.

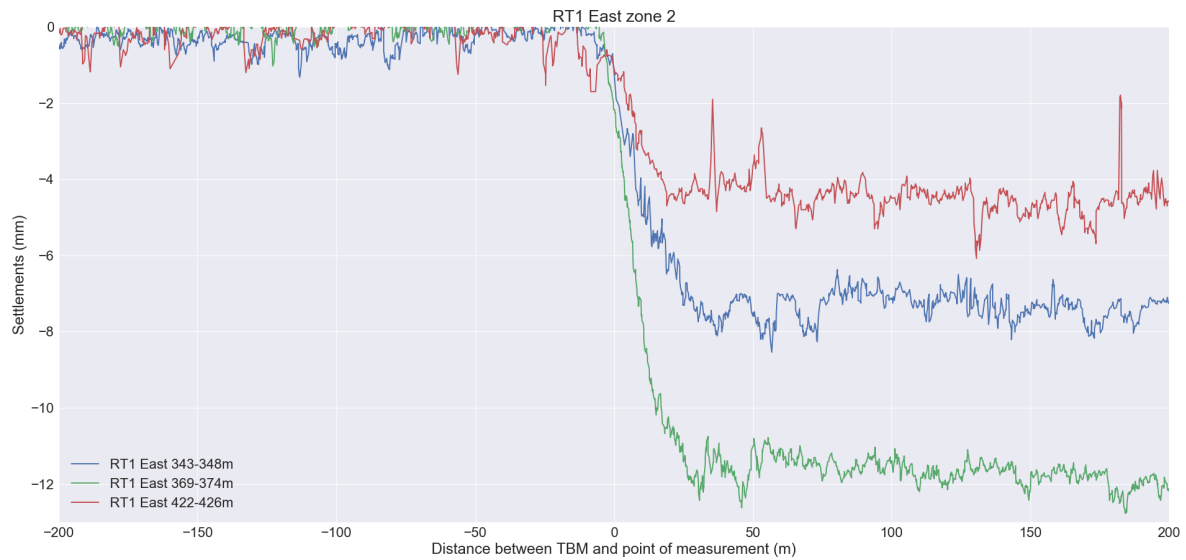


Figure 5.17: Comparison of the average settlement development curves of RT1 East zone 2.



Figure 5.18: Comparison of the normalised average settlement development curves of RT1 East zone 2.

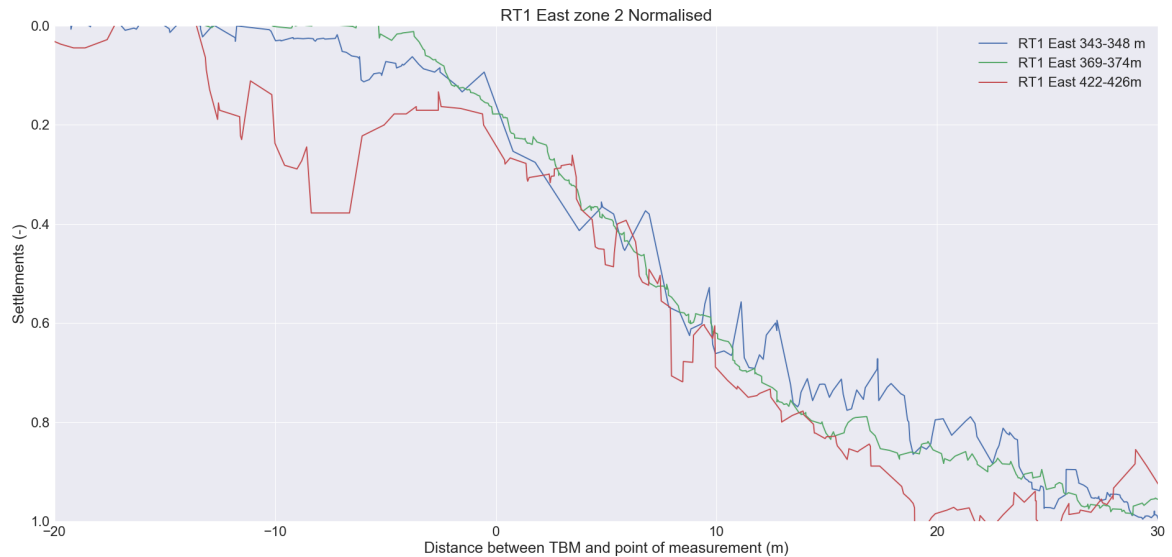


Figure 5.19: Comparison of the normalised average settlement development curves of RT1 East zone 2.

5.4.6. RT1 East zone 3

The settlements in zone 3 of the RT1 East, in figure 5.20, trajectory show very similar maximums. The 630-635 m reaches its maximum earlier however. A better comparison can be found in the normalised settlement development curves in figures 5.21 and 5.22. It can be seen that the 630-635m section already reaches its maximum settlements when the front of the TBM is 12.5 meters past the point of measurement, the 554-560m graph does this at around 19 metres. It has to be kept in mind though that the zone of influence of the 554-560m graph is much bigger as well. That graph starts to settle with the front of the TBM 10 metres before reaching the measurement points, while for the 630-635m graph this is on only 2.5 metres.



Figure 5.20: Comparison of the average settlement development curves of RT1 East zone 3.

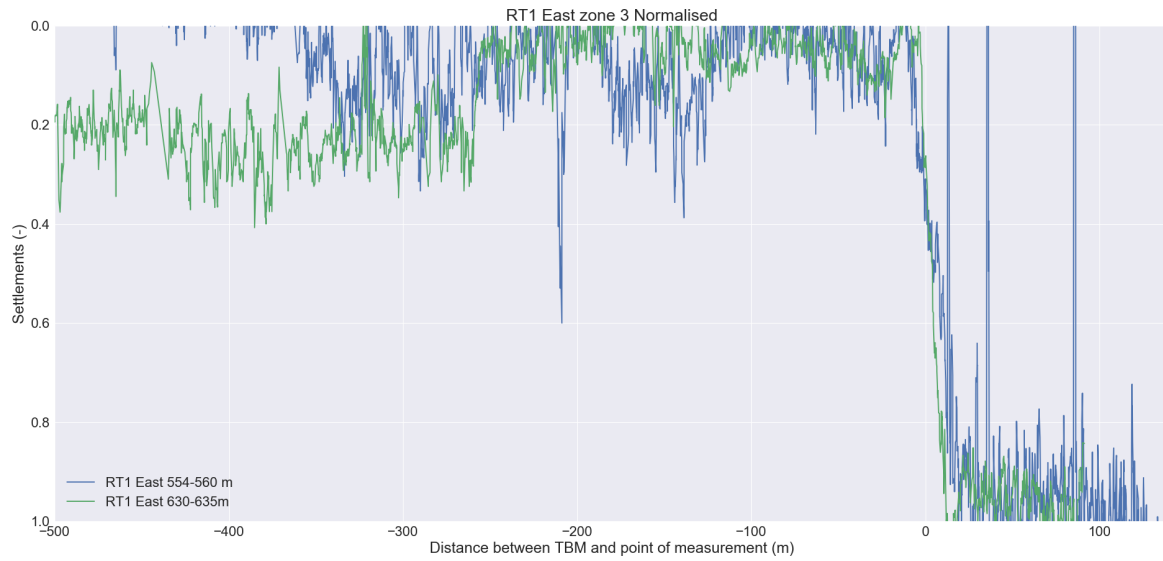


Figure 5.21: Comparison of the normalised average settlement development curves of RT1 East zone 3.

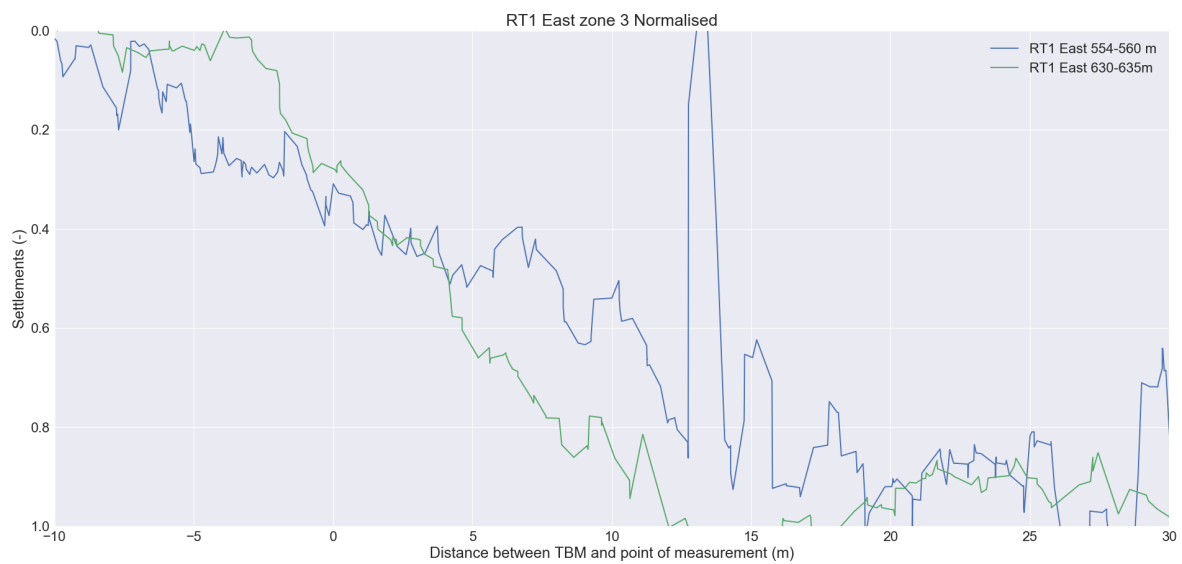


Figure 5.22: Comparison of the normalised average settlement development curves of RT1 East zone 3.

5.4.7. RT4 West zone 1

Looking at figure 5.23 first thing that can be noticed is the consolidation that the 3647-3658m curve undergoes, while the 3572-3577m curve does not. Then looking at the normalised graphs in figures 5.24 and 5.24 it can be seen that the 3572-3577m curve reaches its maximum settlements before the 20m mark while the settlements of the 3647-3658m curve seem to slow down just after 20m. This indicates that there is less influence off the tail void in the total settlements.

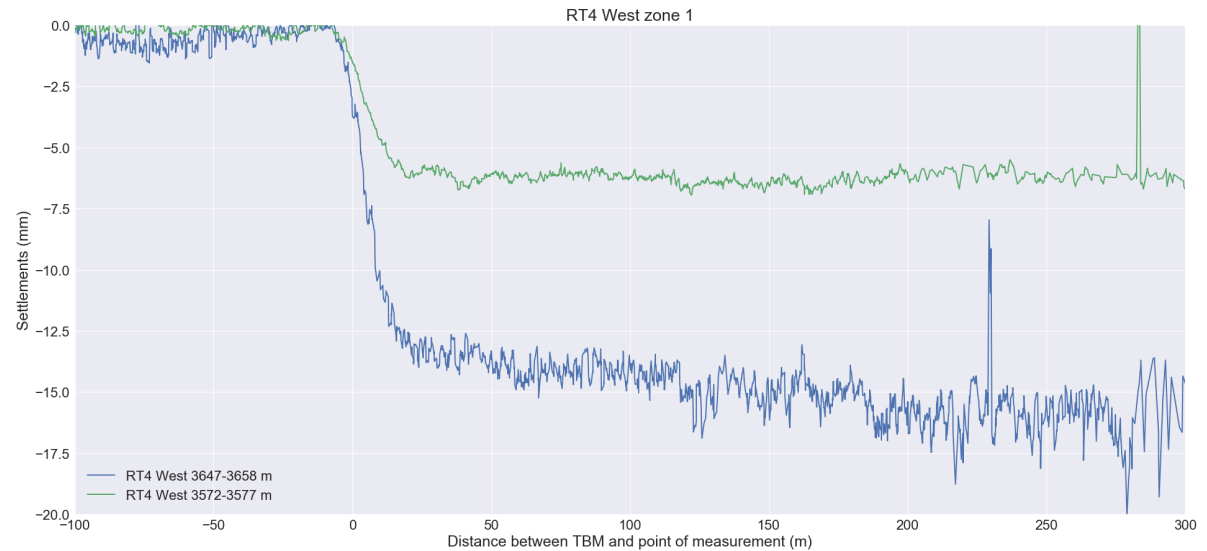


Figure 5.23: Comparison of the average settlement development curves of RT4 West zone 1.

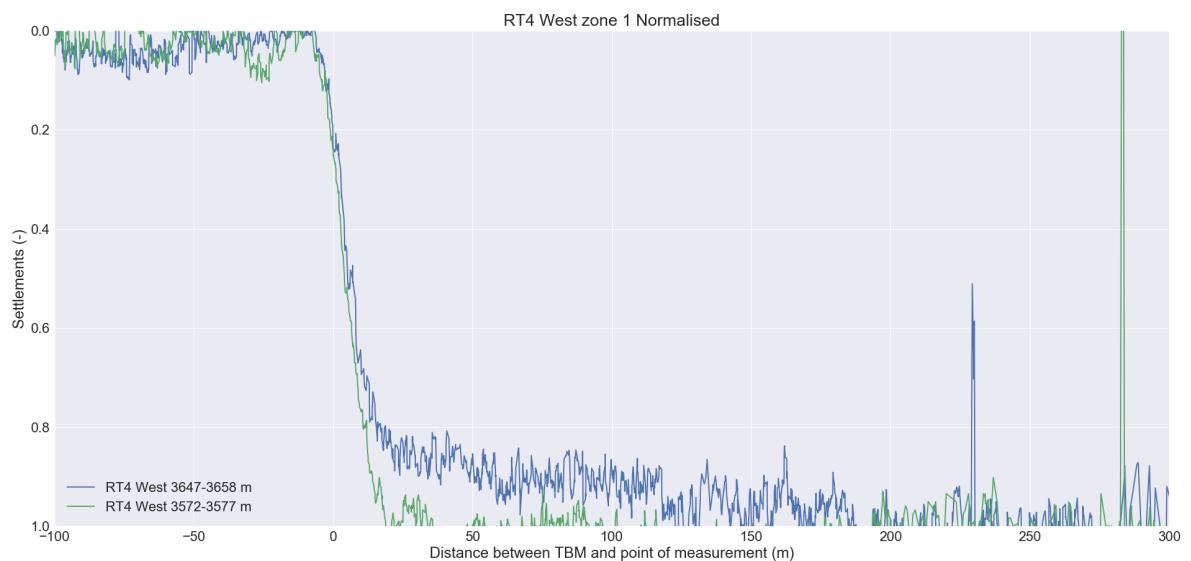


Figure 5.24: Comparison of the normalised average settlement development curves of RT4 West zone 1.

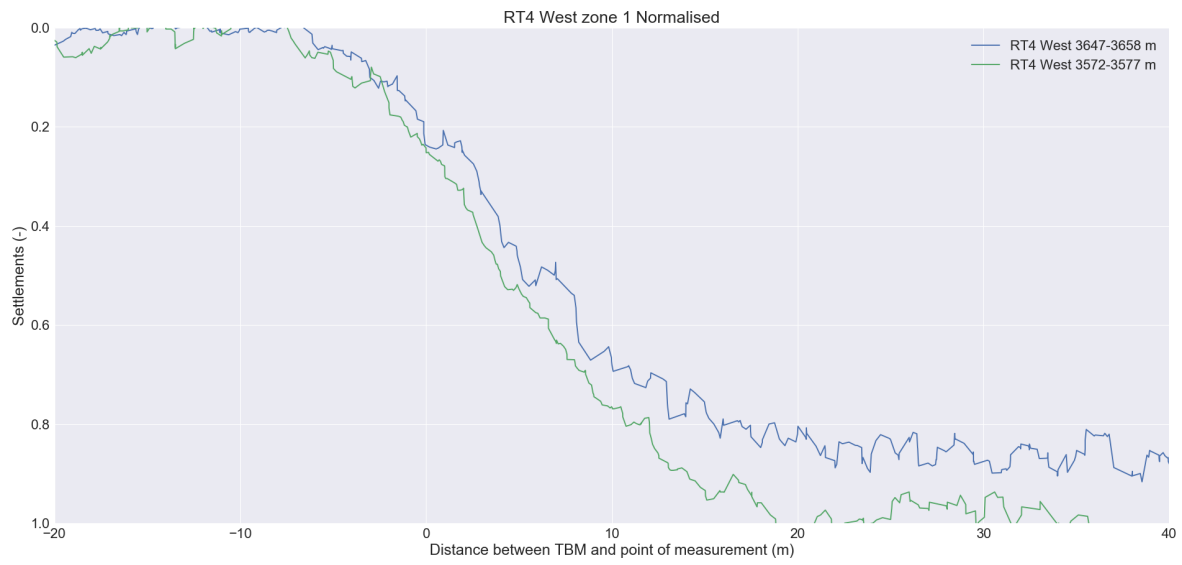


Figure 5.25: Comparison of the normalised average settlement development curves of RT4 West zone 1.

5.4.8. RT4 West zone 2

The settlement development curve of RT1 West zone 2 can be found in figure 5.26, with the 3572-3577m curve having just a little less total settlements. However, looking at the normalised curves in figures 5.27 and 5.27 it can be seen that the 3572-3577m stop settling before the front of the TBM passed by 20m while the 346-3443m graph keeps settling until the TBM has passed for almost 40 meters.



Figure 5.26: Comparison of the average settlement development curves of RT4 West zone 2.

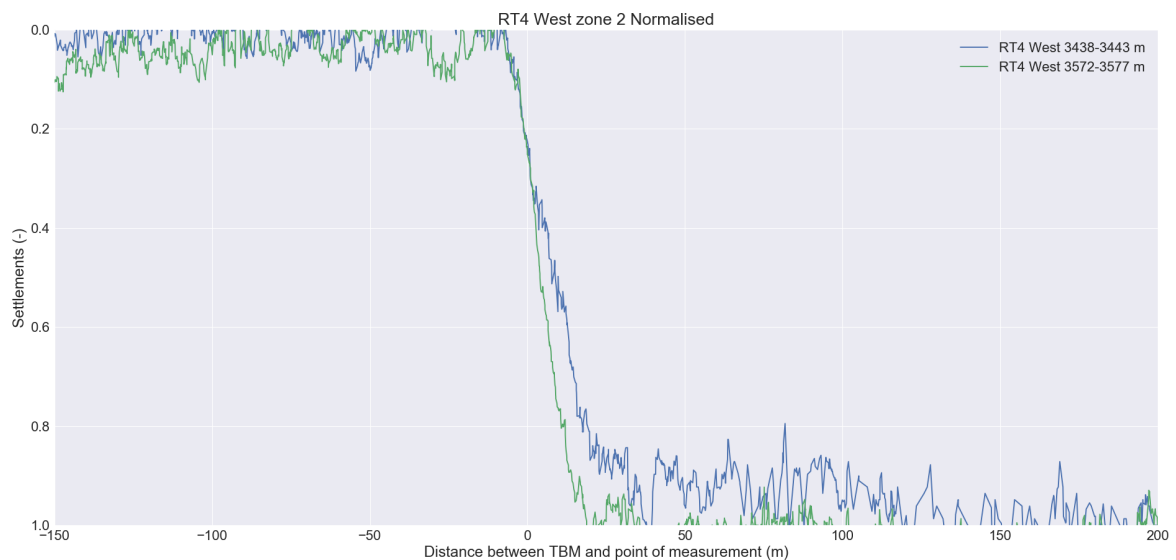


Figure 5.27: Comparison of the normalised average settlement development curves of RT4 West zone 2.

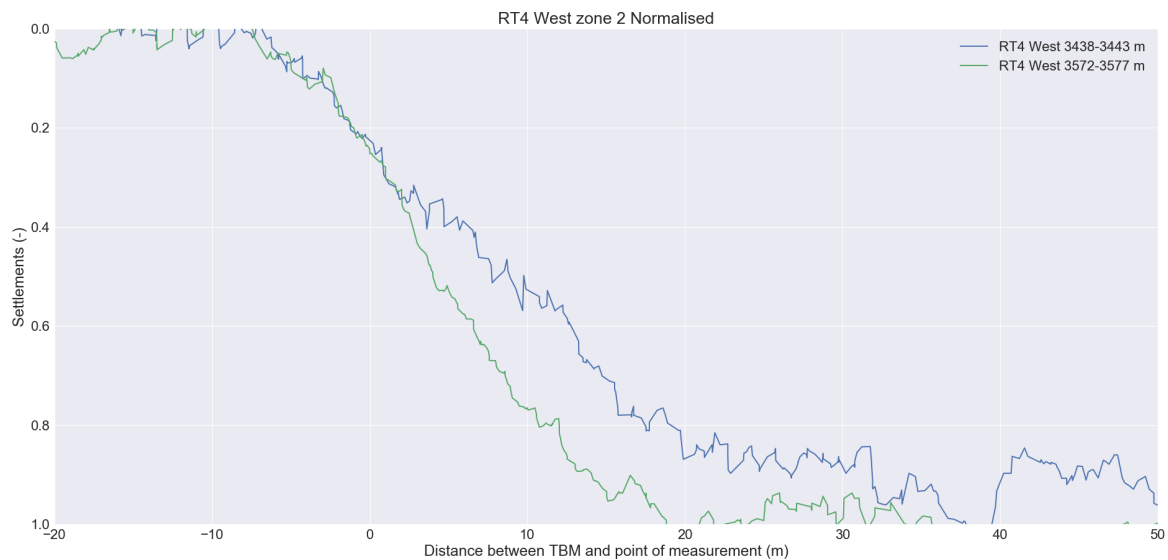


Figure 5.28: Comparison of the normalised average settlement development curves of RT4 West zone 2.

5.4.9. RT4 West zone 3

RT4 West zone 3 consists of three curves, figure 5.29, one of these reaches a total settlement of only 3 mm while the other 2 reach a total settlements of 6.5mm. The problem with having this little settlement can clearly be seen in the normalised curves in figure 5.30 and 5.31. All of the curves look very similar and are hard to compare due to the big amount of noise caused by the fact that the total settlements are not that much bigger than the noise resulting in the noise causing problems in the normalised graphs.



Figure 5.29: Comparison of the average settlement development curves of RT4 West zone 3.



Figure 5.30: Comparison of the normalised average settlement development curves of RT4 West zone 3.

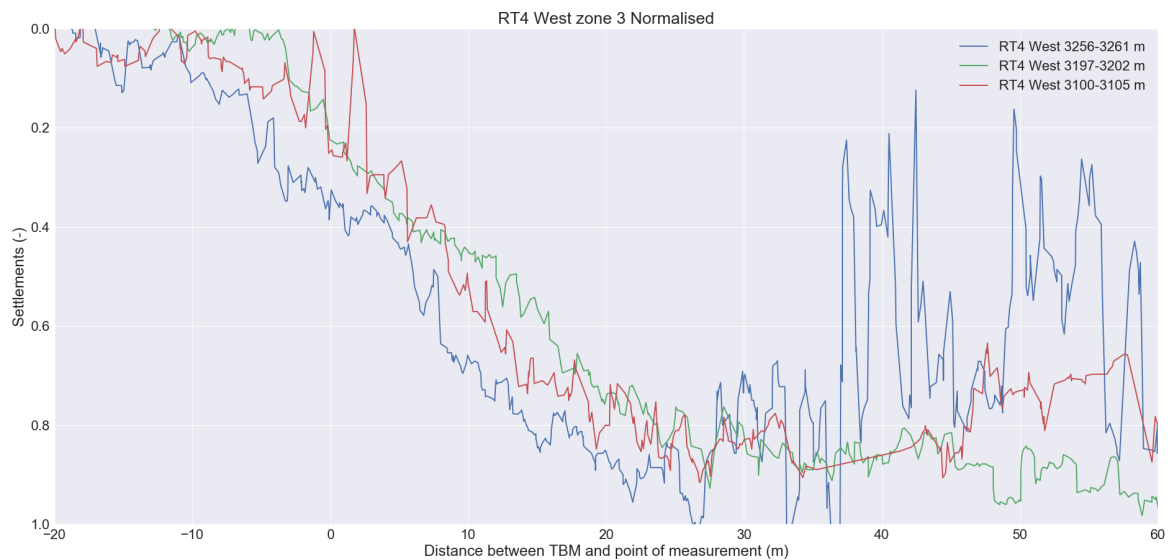


Figure 5.31: Comparison of the normalised average settlement development curves of RT4 West zone 3.

5.4.10. RT4 East

For the RT4 East section 3 settlement development curves are created and shown in figure 5.32. Two of these reach a total settlement between 5 and 6 mm while the other location reaches a total settlement of just over 10mm of settlements. In the normalised graphs in figures 5.33 and 5.34 it can be seen that the 3188-3194m curve stops settling first, whereafter secondly the 3262-3267m curve stops settling to finally have the 3455-3460m curve to stop settling.



Figure 5.32: Comparison of the average settlement development curves of RT4 East.

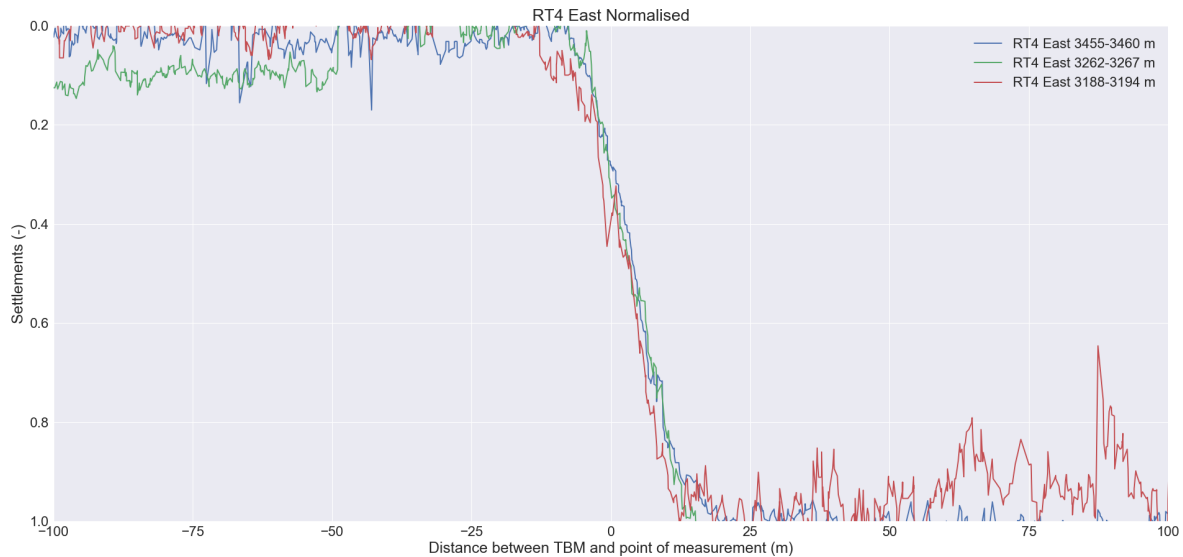


Figure 5.33: Comparison of the normalised average settlement development curves of RT4 East.



Figure 5.34: Comparison of the normalised average settlement development curves of RT4 East.

5.5. Discussion

This chapter illustrated the influence of the tail void on the settlements. The grouting behaviour and the distance between the front of the TBM and the point of measurement at the moment the total settlements are reached, is shown in figure 5.35. Here, the moment that the soil stops settling is used as an indicator for the tail void performance. No relation is found here. It has to be kept in mind that when comparing these locations, a lot of parameters influencing the settlements and its development were ignored, as tunnels of different depths and at different locations were compared. Apparently these influence the zone of influence so much that it is not possible to find a direct relation. To overcome this problem tunnels that are closer to each other are compared qualitatively. Table 5.1 shows the outcome of this chapter with the corresponding locations. Here it can be seen that when comparing two locations nearby each other, a higher grout volume leads to a better performing tail void (in grey). The grout pressures do not show any relation with the performance of the tail void. Note that the total settlements do not have to improve by the grouting of the tail void as the grouting does not have any influence on the settlements induced by other components of the TBM.

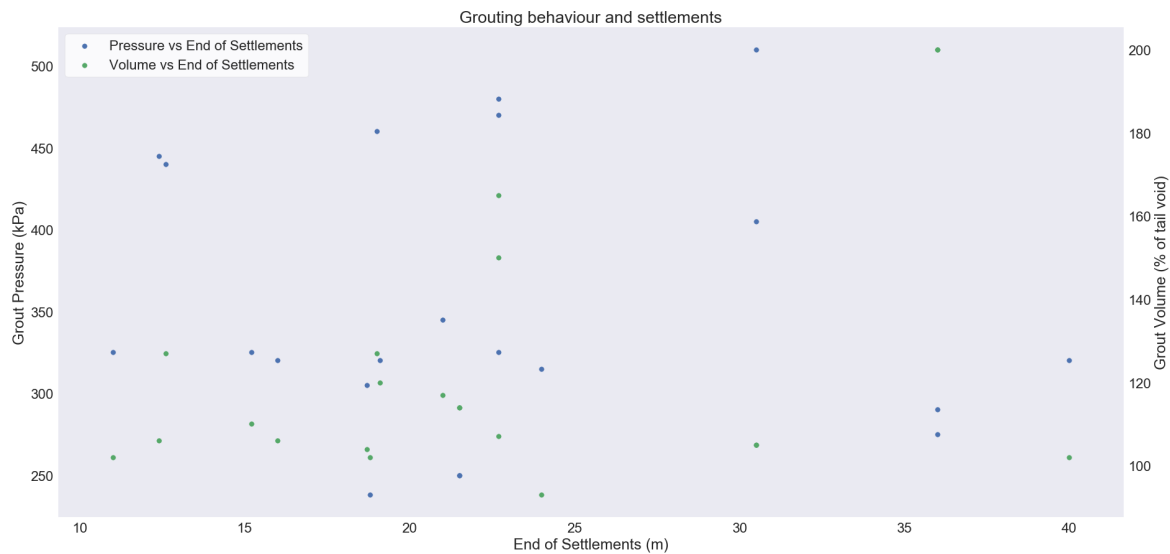


Figure 5.35: Scatter plot of the grout pressures in the tail void (left y axis) and the grout volumes injected in the tail void (right y axis) against the distance between the front of the TBM and point of measurement at the moment the total settlements are reached.

Table 5.1: Overview of settlement graphs and grouting behaviour.

Location	Contains (m)	Settlements	Normalised settlement	Grout Pressure	Grout Volume
RT1W1	A: 101-109	A>B	Equal	B>A	A>B
	B: 112-117				
RT1W2	A: 187-195	A>B	Tail B performs better than tail A	A=B	B>A
	B: 203-211				
RT1W3	A: 580-585	B>A	B shows a smaller zone of influne than A	A=B	A=B
	B: 650-656				
RT1E1	A: 173-180	B>A=C	Equal	C>A=B	B=C>A
	B: 197-203				
	C: 212-219				
RT1E2	A: 343-348	B>A>C	Tail C performs better than the other 2	C>B>A	C>A=B
	B: 369-374				
	C: 422-426				
RT1E3	A: 554-560	A=B	Tail B performs better than A	B>A	B>A
	B: 630-635				
RT4W1	A: 3647-3658	B>A	Tail B performs better than A	A=B	B>A
	B: 3572-3577				
RT4W2	A: 3438-3443	A>B	Tail B performs better than A	A>B	B>A
	B: 3572-3577				
RT4W3	A: 3256-3261	B=C>A	Incomparable	B>C>A	A=B>C
	B: 3197-3202				
	C: 3100-3105				
RT4E	A: 3455-3460	A>B>C	Equal	C>B>A	A=B=C
	B: 3262-3267				
	C: 3188-3194				

Settlements, $A > B$ = Region A had more settlements than region B

Grout Pressure, $A > B$ = Pressures in region A were bigger than in region AB

Grout Volume, $A > B$ = In region A a higher grouting volume was used than in region B

Grout- and soil pressures in the tail void

The direct comparison between the grout pressures and the settlements in chapter 4 ignored an important factor: the stress of the surrounding soil. The radial stress of the soil towards the tail void causes the soil to collapse into the void. To overcome this problem, the grout in the tail void is supposed to 'carry' the soil. As soon as the tail void is completely filled the grout particles can fulfil that role. However, until that moment, the grout pressures are expected to do so. Chapter 5 showed several locations where the tail void was responsible for the change in settlements. For these locations the grout pressures are visualised together with the soil pressure in an attempt to find a relation between the grout pressures in the tail void and the induced settlements.

6.1. Methods

Polar plots visualise the grout pressure in the tail void and the soil pressure in one figure. The soil pressure was measured at 6 measuring points at the back of the TBM in the tail void (see section 3.1), numbered 1 to 6 in the figures. In between these points, the pressures are linearly interpolated over the height difference in the tail void, resulting in a curved line in the polar plot. Occasionally, these sensors measured pressures lower than the surrounding pore water pressures. As the pore water around the tail void can probably enter the tail void the pore pressure of the surrounding soil is expected to be the minimum pressure in the tail void. Therefore, when the measured grout pressures drop below the water pressure, these are corrected to the level of the local water pressure.

The grout pressures varies a lot during the boring process. When the TBM starts boring and it is filling the tail void with grout, the pressure increases. When the boring stops, whether it is because the ring building starts or there is a standstill caused by a problem, the grouting of the tail void stops as well. The flow of water out of the grout into the surrounding soil causes the pressures to drop again (see chapter 7). To visualise every part of this process, polar plots are made for 100 moments during the entire boring process. In an attempt to find a relation to the pressures in the tail void and the induced settlements the pressures in the tail void are compared before and after the changes in the settlements for the locations selected in chapter 5.

6.2. RT1 zone 2

Zone 2 of the RT1 section is located around the 200 meter mark (see figure 4.9). The western trajectory shows a sudden decrease in settlements, while the eastern trajectory shows a short dip in the settlements whereafter the settlements recovers to the level of before the dip. At the same time the western trajectory shows an increase in grout volume paired with a temporary increase in the grout pressure which then dropped back to its old level. For the eastern trajectory the used grout volumes are, at 200m, still dropping from the extreme high levels that were used the first 100 metres underneath the frozen soil. The pressures however increases.

Paragraph 5.4.2 indicates that the performance of the tail void causes the decrease in settlements at this location. For the east side paragraph 5.4.4 shows that normalised curves of before, after and during the dip in settlements look exactly the same, indicating that the settlement change is not initiated by a change in TBM behaviour.

The 200 meter mark is reached by both tunnels by the 134th ring. Since paragraph 5.4 shows that the ring not only influences the settlements directly above it but also slightly further away. Therefore multiple rings

are analysed before, on and after the 200m mark. The eastern rings are numbered 1000-1478 and the western rings 2000-2481, e.g. ring 134 is numbered 1134 and 2134 resp.. Note that the data is stored under the number of the drilled ring and the measurements of the tail void pressures is at the back of the TBM. Therefore the location of the measured is actually the length of the shield of the TBM, 7m, further back as the ring number the data shows. For example the data at the 200m mark is not the data from ring 134 but the data from ring 138.

6.2.1. RT1W2

This section compares the pressures in the tail void before and after the change in settlements to investigate a possible relation between those pressures and the settlements. The change in settlements is located just before 200m. If the settlements would be caused by a change in grout pressures a difference in grout pressures should be observed before and after a settlement change.

Figures 6.1-6.3 show the measured grout pressures at 3 times during the boring process: at the beginning of the boring of ring number 130, at the beginning of the ring building phase and at the end of the ring building process. The pressure at the beginning of the bore process are lower than the local soil pressure at sensors 4 and 6. Then at the end of the bore process the pressures rise due to the injection of the grout during the boring. To finally decrease again during the building of the ring, when no grout is added to the tail void.

If the grout pressures are the cause of the change in settlements a different behaviour is expected after this change in settlements. Figures 6.4-6.6 show the pressures in the tail void during the boring of ring 143 of RT1 West. Here, the pressures also are lower than the soil pressure during the beginning of the boring process. Then, at the beginning of the ring building process the pressure at sensor 4 is significantly higher than at ring number 130, while the pressures at the other sensors are comparable. Then, at the end of the ring building phase the pressure at the top of ring 143 are actually lower than the ones found during the drilling of ring 130.

Ring no.:2130 time since start boring: 0.01 h

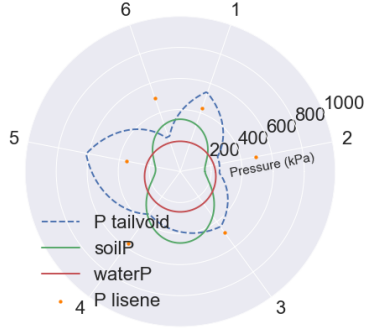


Figure 6.1: Polar representation of the grout pressures in the tail void at the beginning of the boring phase of ring 130 at the RT1 West trajectory.

Ring no.:2143 time since start boring: 0.01 h

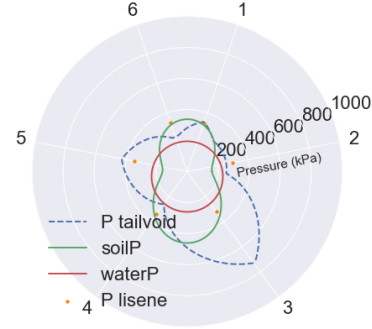


Figure 6.4: Polar representation of the grout pressures in the tail void at the beginning of the boring phase of ring 143 at the RT1 West trajectory.

Ring no.:2130 time since start boring: 0.41 h

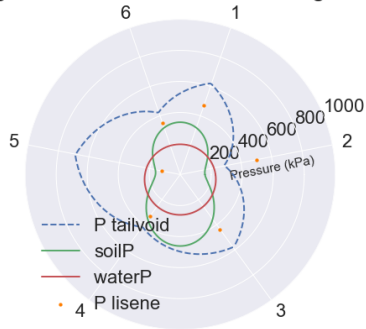


Figure 6.2: Polar representation of the grout pressures in the tail void at the beginning of the ring building phase of ring 130 at the RT1 West trajectory.

Ring no.:2143 time since start boring: 0.52 h

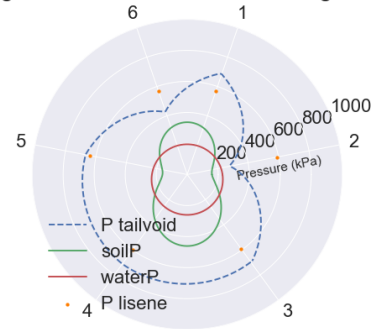


Figure 6.5: Polar representation of the grout pressures in the tail void at the beginning of the ring building phase of ring 143 at the RT1 West trajectory.

Ring no.:2130 time since start boring: 2.49 h

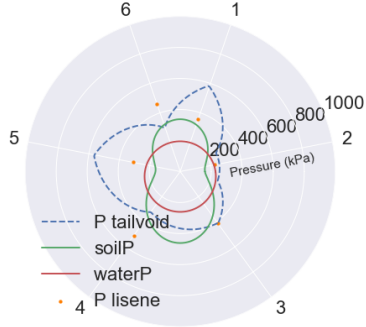


Figure 6.3: Polar representation of the grout pressures in the tail void at the end of the ring building phase of ring 130 at the RT1 West trajectory.

Ring no.:2143 time since start boring: 1.48 h

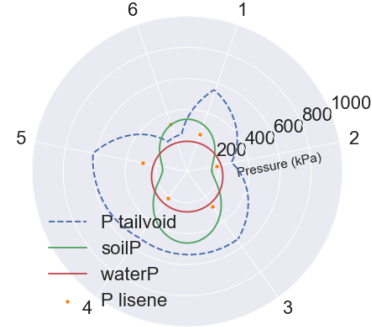


Figure 6.6: Polar representation of the grout pressures in the tail void at the end of the ring building phase of ring 143 at the RT1 West trajectory.

6.2.2. RT1E2

In the comparison of RT1E2 three locations are taken into account. The first location is located before a drop in settlements, the second is located at the bottom of this dip while C is located while the settlements are restored to their old level. Table 5.1 shows that the tail of location C performs better than the other two. Figures 6.7-6.15 show the grouting pressures at these locations. Both 252 and 287 show higher pressures in the tail void than 234. However it is hard to tell whether 252 or 287 shows higher pressures since they peak at different locations. From this 3 locations 287, the better performing location tail void inducing settlement wise, is the only location that shows pressures under the ground pressure.

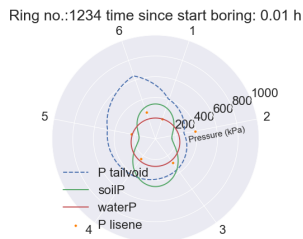


Figure 6.7: Polar representation of the grout pressures in the tail void at the beginning of the boring phase of ring 234 at the RT1 East trajectory.



Figure 6.10: Polar representation of the grout pressures in the tail void at the beginning of the boring phase of ring 252 at the RT1 East trajectory.



Figure 6.13: Polar representation of the grout pressures in the tail void at the beginning of the boring phase of ring 287 at the RT1 East trajectory.

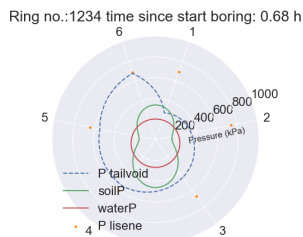


Figure 6.8: Polar representation of the grout pressures in the tail void at the beginning of the ring building phase of ring 234 at the RT1 East trajectory.

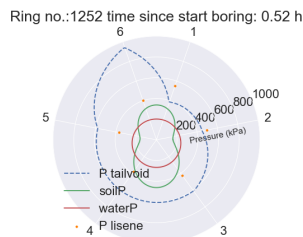


Figure 6.11: Polar representation of the grout pressures in the tail void at the beginning of the ring building phase of ring 252 at the RT1 East trajectory.

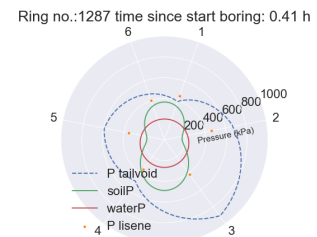


Figure 6.14: Polar representation of the grout pressures in the tail void at the beginning of the ring building phase of ring 278 at the RT1 East trajectory.

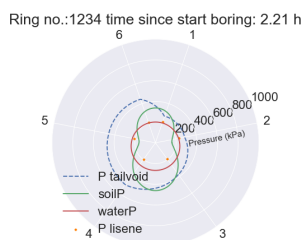


Figure 6.9: Polar representation of the grout pressures in the tail void at the end of the ring building phase of ring 234 at the RT1 East trajectory.

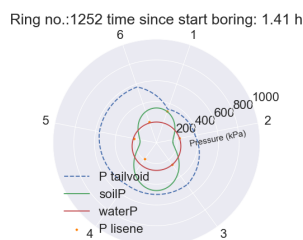


Figure 6.12: Polar representation of the grout pressures in the tail void at the end of the ring building phase of ring 252 at the RT1 East trajectory.

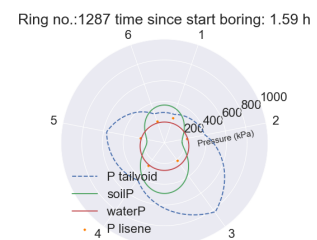


Figure 6.15: Polar representation of the grout pressures in the tail void at the end of the ring building phase of ring 278 at the RT1 East trajectory.

6.2.3. RT1E3

The 630-635 area shows better performance in the tail void settlements than the 554-560m area, as seen in chapter 5. Table 5.1 shows also that the pressure and the grout volume are higher in the 630-635m area. Figures 6.16-6.21 show the evolution of these pressures during all of the boring phases. The grout pressures of ring 375, in the 554-560m area, are very low compared to the pressures of ring 426, in the 630-635m area, at all times.

Ring no.:1375 time since start boring: 0.01 h

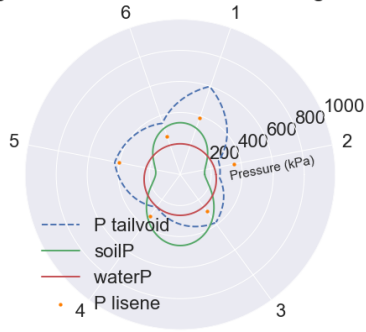


Figure 6.16: Polar representation of the grout pressures in the tail void at the beginning of the boring phase of ring 375 at the RT1 East trajectory.

Ring no.:1426 time since start boring: 0.02 h

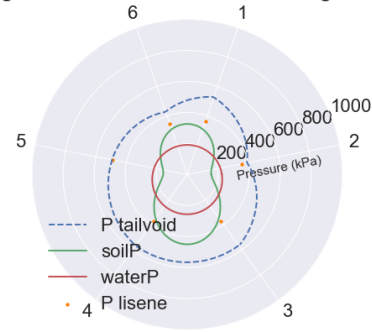


Figure 6.19: Polar representation of the grout pressures in the tail void at the beginning of the boring phase of ring 426 at the RT1 East trajectory.

Ring no.:1375 time since start boring: 0.54 h

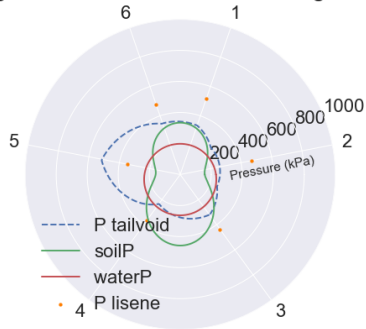


Figure 6.17: Polar representation of the grout pressures in the tail void at the beginning of the ring building phase of ring 375 at the RT1 East trajectory.

Ring no.:1426 time since start boring: 0.51 h

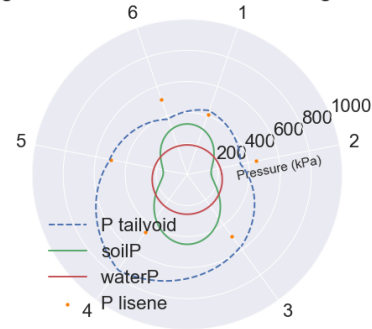


Figure 6.20: Polar representation of the grout pressures in the tail void at the beginning of the ring building phase of ring 426 at the RT1 East trajectory.

Ring no.:1375 time since start boring: 2.46 h

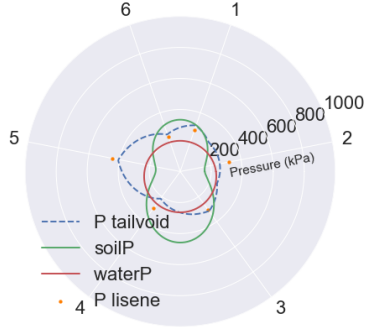


Figure 6.18: Polar representation of the grout pressures in the tail void at the end of the ring building phase of ring 375 at the RT1 East trajectory.

Ring no.:1426 time since start boring: 4.47 h

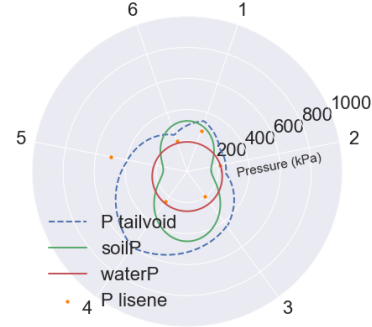


Figure 6.21: Polar representation of the grout pressures in the tail void at the end of the ring building phase of ring 426 at the RT1 East trajectory.

6.2.4. RT4W

The RT4 section contains two zones where the tail void of one location performs better than the other. However, as these two zones share one location (the 572-577m) they are combined. This results in the three locations shown in figures 6.22-6.30. Here, the first thing that jumps out is the extremely high pressures at sensor 1 of ring numbers 140 and 230. These are not actual high pressures but is due to a broken sensor. Also, the pressures of all the three rings are low and comparable. Only ring 230 shows a higher pressure at the third sensor than the other two. Table 5.1 shows that ring 140 is the one with the better performing tail void.

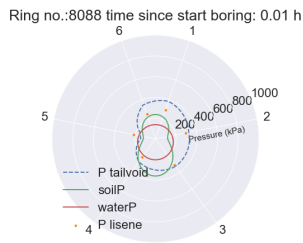


Figure 6.22: Polar representation of the grout pressures in the tail void at the beginning of the boring phase of ring 88 at the RT4 West trajectory.

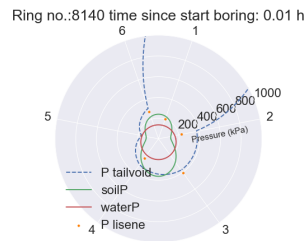


Figure 6.25: Polar representation of the grout pressures in the tail void at the beginning of the boring phase of ring 140 at the RT4 West trajectory.

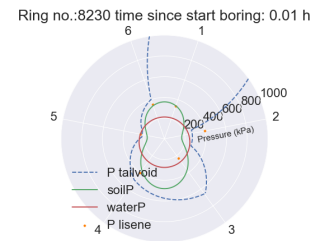


Figure 6.28: Polar representation of the grout pressures in the tail void at the beginning of the boring phase of ring 230 at the RT4 West trajectory.

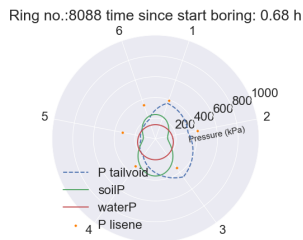


Figure 6.23: Polar representation of the grout pressures in the tail void at the beginning of the ring building phase of ring 88 at the RT4 West trajectory.

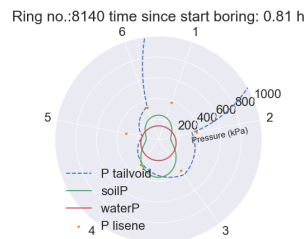


Figure 6.26: Polar representation of the grout pressures in the tail void at the beginning of the ring building phase of ring 140 at the RT4 West trajectory.

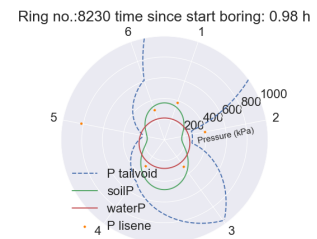


Figure 6.29: Polar representation of the grout pressures in the tail void at the beginning of the ring building phase of ring 230 at the RT4 West trajectory.

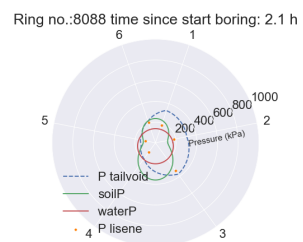


Figure 6.24: Polar representation of the grout pressures in the tail void at the end of the ring building phase of ring 88 at the RT4 West trajectory.

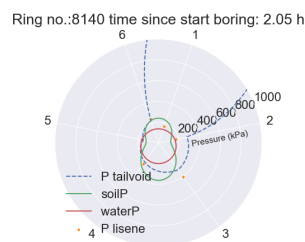


Figure 6.27: Polar representation of the grout pressures in the tail void at the end of the ring building phase of ring 140 at the RT4 West trajectory.

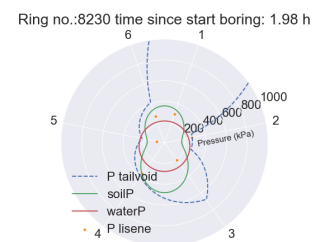


Figure 6.30: Polar representation of the grout pressures in the tail void at the end of the ring building phase of ring 230 at the RT4 West trajectory.

6.3. Discussion

The goal of this chapter was to further investigate the possible relationship between the grout pressure in the tail void and the settlements. Two locations showed higher pressures where the tail void of the TBM performed better. However, at one location the pressure stayed at a comparable level and in the fourth location, the grout pressure even showed an inverse relation as these were lower. This given, combined with the results of chapter 4, indicates that there is no proven relation between the grout pressure in the tail void and the settlements.

Dissipation of the grout pressures during TBM standstill

The grout injection in the tail void during the forward movement of the TBM causes the grout pressure to rise. When the TBM comes to a stop, the grout injection stops and the pressure starts to drop. This chapter analyses the development and dissipation of the grout pressure in the tail void.

7.1. Methods

Paragraph 2.3.2 showed the influence of the permeability of the surrounding soil on the rate of dissipation of the grout pressure in the tail void. This chapter aims to apply this theory to the case of the North/South line. To do so, rings in multiple surroundings are compared. The first ring is bored in the permeable second sand layer and the second ring is bored in the impermeable Eemclay. To assess whether different dissipation rates are occurring, the development of the grout pressure is compared during the ring building phase of the TBM. Here it is assumed that during the ring building phase, the volume of the tail void stays constant. This means that if there is no outflow of water, no additional grout injection and the volume of the tail void stays constant, the grout pressure stays constant. In this case, the tail void volume is constant so as soon as no further grout is injected, any variation of the grout pressure is caused by the outflow of the water into the soil.

7.2. Dependency of the grout pressure dissipation on the surrounding soil

Figure 7.1 shows the dissipation of the grout pressure in the Eemclay. The Eemclay has a permeability of $1 \cdot 10^{-9}$ m/s. Figure 7.2 shows the dissipation of the grout pressure in the second sand layer. This sand has a permeability of $1 \cdot 10^{-4}$ m/s. A comparison of the figures illustrates that the dissipation of grout pressure happens much quicker in the sand than in the Eemclay. Although the grout pressure does dissipate in the clay layer, it happens so slowly that there enough time to build up the tunnel ring and still maintain a grout pressure that is not significantly lower than its original value. In the sand layer, a rather quick drop in grout pressure occurs as soon as grouting stops at the end of the boring phase. The fact that grout pressure in the Eemclay drops slower than in the sand, shows that the outflow of water is slower in the clay than in the sand.

7.3. Discussion

The quick drop in grouting pressure shows that it is difficult to maintain grout pressure in the tail void when drilling in sand. During the pressure dissipation, only the fluid in the grout mixture flows out into the soil, this means the solids stay behind in the tail void. When this process continues, the tail void fills up with the solids in the grout, forming a soil like grain skeleton preventing the tail void from collapsing.

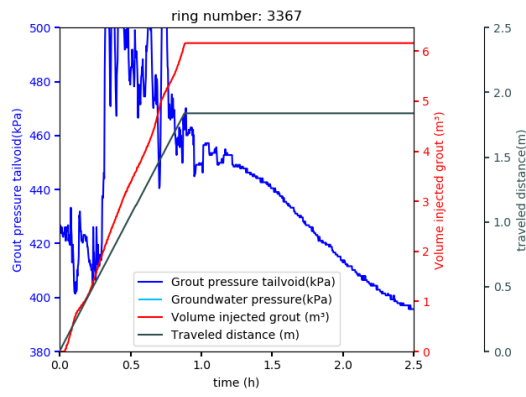


Figure 7.1: Grout pressures during drilling and stand still in clay(here the groundwater pressure under the bottom of the graph and is 250 kPa

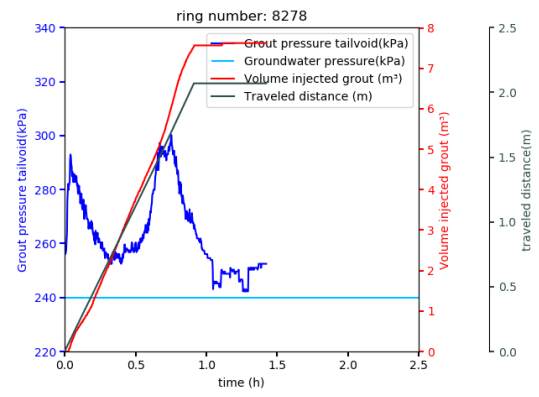
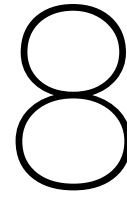


Figure 7.2: Grout pressures during drilling and stand still in sand



Finite Element Model validation

A limitation of the data analyses executed in earlier chapters of this thesis, is that the input data could not be modified. As multiple parameters change at the same time, it is difficult to isolate the effect of one single parameter. In Finite Element Modelling (FEM) it is possible to change one parameter at a time, making it possible to analyse its direct effect. The FEM method is used to model the RT1 trajectory of the North/South line tunnel in DIANA. The model is then used to analyse the effect of the tail void on the total settlements.

8.1. Methods

The model consists of 9 soil layers matching the stratigraphy of the RT1 trajectory (figure 8.1). The soil is divided in 3 groups and modelled as a hardening soil model. The biggest group consists of the entire model except for a rectangular cuboid in the middle of the model. The inner cuboid consists of the other two soil groups sliced at the location the tunnel rings are later placed (figure 8.2). This way, it becomes possible to excavate the tunnel ring by ring, simulating the behaviour of the TBM. The model is 75 meter long, which is the length of 50 rings, 90 meter wide and 46 meter deep with the top of the tunnel located 21 meters underneath the surface.

The tunnel is build step-wise. During every step, the soil volume excavated by the TBM (the size of 1 ring) is deactivated. On this location, a rigid support is placed, mimicking the TBM shield. With the use of an interface, the shield support is connected with the surrounding soil. This interface contains a fictive gap to represent the tapering of the TBM. The next slice of soil is supported with a rigid face support. As the TBM moves forward, the next soil slice is deactivated and again, the TBM support is placed. The fictive gap on the interface is increased every step, simulating the tapering of the moving TBM. After the processing of four rings, the 1 cm gap at the tail of the TBM is reached. Hereafter, the lining is placed at that location. The lining consists of six segments that are connected with couplers and plates. In the FEM, the couplers are modelled as springs and plates are modelled as point interfaces that simulate friction. At the outside of the lining, an interface is placed which connects the segments with the surrounding soil. This interface contains a fictive gap of 180mm, simulating the tail void. A pressure is applied to both sides of the interface to simulate the liquid grout supporting the tail void. Then, after a few rings, the interface is removed as in reality, the grout would have hardened, stopping the soil from moving into the gap.

8.2. Varying the grout pressures

The effect of the settlements of the tail void on the total settlements is checked by varying the applied pressures behind the TBM. Three different calculations are run: one with a pressure of 200 kPa, one of 400 kPa and one of 600 kPa. A Comparison of these results gives an indication of the influence of the tail void on the total settlements. Figure 8.3 shows the induced settlements for the 400 kPa calculation. The settlement development curves of the middle of the model are visualised in figure 8.4. These curves show that the difference in total settlements between the highest and the smallest pressure is only 4 mm. Furthermore, when only the pressure in the tail void varies, the settlement curves start to diverge around 15 meters before the front of the TBM passes the point of measurements. This effect increases as the tail void comes closer to the point of measurement.

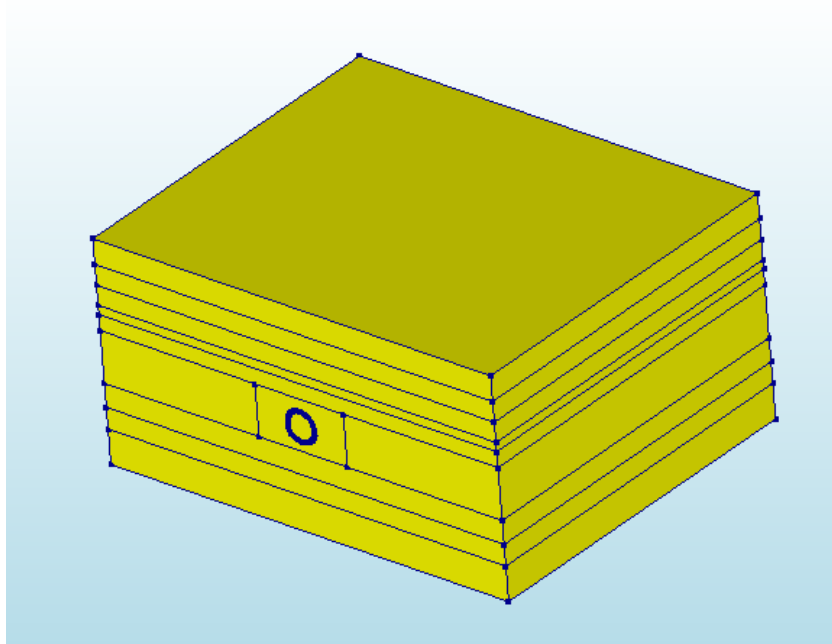


Figure 8.1: Overview of the FEM model.

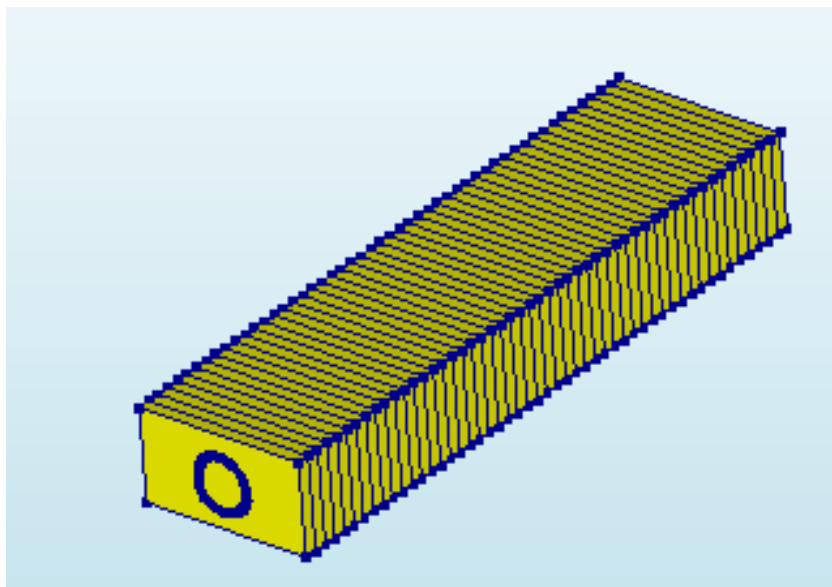


Figure 8.2: Inner soil of the FEM model.

8.3. Discussion

The outcomes of the FEM calculations illustrate that a difference in tail void behaviour showed its effects already at 15 meters in front of the TBM, this is 22 meter in front of the start of the tail void. Combining this with the fact that the difference in settlements turned out to be only 4 mm, emphasises how difficult it is to isolate the settlements induced by the tail void and why no direct relation could be found between the the grouting process and the total settlements.

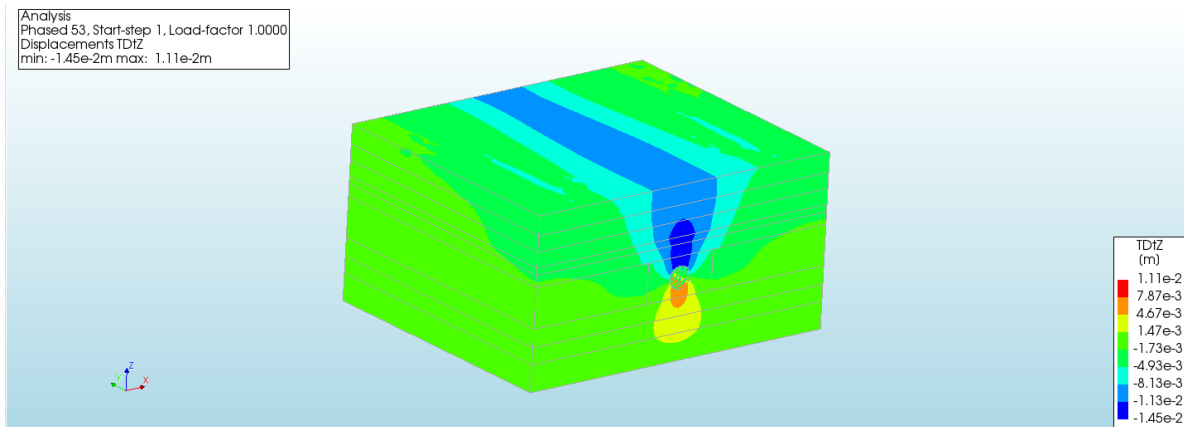


Figure 8.3: Overview of the settlements induced by the FEM model at 400kPa

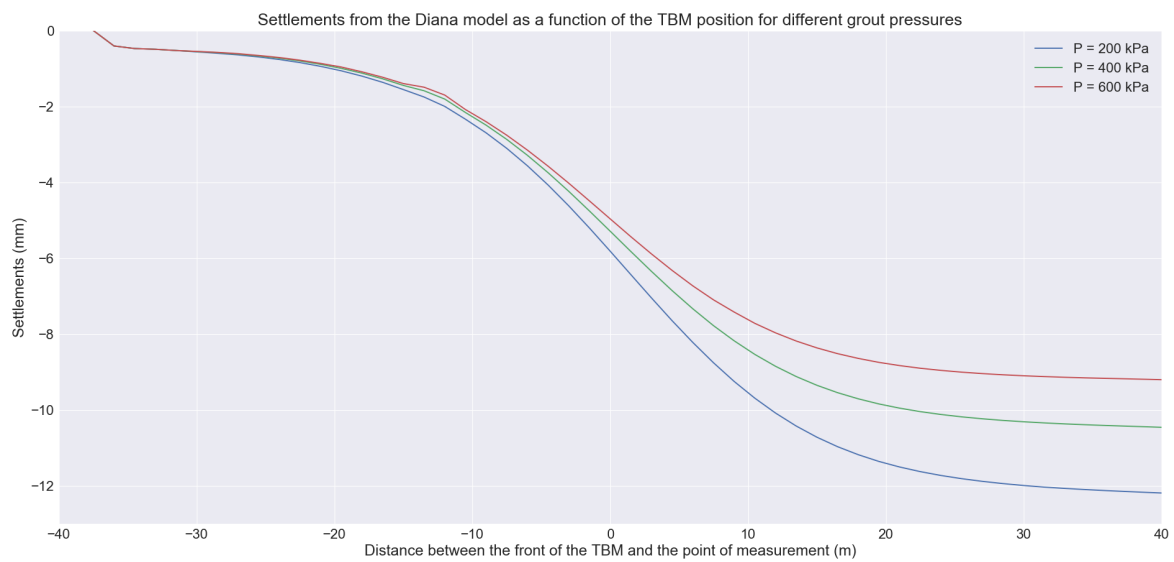


Figure 8.4: Overview of the FEM model

Discussion and Conclusions

9.1. Main findings

To find the answer on the formulated research questions, this thesis research was build up of several steps:

- A background on the subjects of tunnel boring, settlement during TBM passage, grouting of the tail void and the tail void injection test for the North/South line was provided in chapter 2.
- The boundary conditions provided by the case study of the North/South line was presented in Chapter 3.
- The total settlements over the four tunnel trajectories were analysed in chapter 4. The comparison of the injected grout volumes and pressures in the tail void with the changes in the settlements, illustrated that some of the changes in the settlements coincided with changes in the injected grout volume and/or the grout pressure. However, as this was not consistently detectable for all trajectories, no direct relation could be proven.
- The analysis and isolation of the settlements induced by the tail void formed the focus of chapter 5. The settlements were plotted as a function of the TBM position. This way, the curves indicated which component of the TBM was responsible for the settlements. However, the evolution of the settlements was still difficult to compare between locations of different total settlements. Therefore, the curves were divided by their total settlements, creating normalised settlement development curves. Comparing nearby locations with these normalised settlements illustrated that at a part of the locations, the change in settlement was at least partly caused by the tail void. For all of these locations, the tail void induced less settlements where a bigger grout volume was injected. No direct relation was found between the tail void induced settlements and the grout pressure.
- The possible relation between the tail void induced settlements and the grout pressure was further investigated in chapter 6.
- A side step was made with a research into the development of the grout pressure in the tail void in chapter 7. The development of the grout pressure was compared with the different boring phases of the TBM over time. This illustrated that the grout pressure increased during the injection of grout during the boring phase. However, as the TBM stood still to build a new tunnel ring and grout injection stops, the grout pressure dropped. The rate of the pressure drop depends on the permeability of the surrounding soil. Additionally, the grout pressure in the tail void is much lower underneath a frozen soil canopy, pointing towards an influence of the soil pressure on the grout pressure.
- A Finite Element Method (FEM) calculation was provided in chapter 8. This showed that the tail void of the TBM is responsible for only a small part of the total settlements. The difference in total settlements between a very good and a very bad performing tail void is only 3 mm.

9.2. Discussion

Above findings show no direct relation between the total settlements and either the grout volume injected in the tail void or the pressure of that injected grout. Moreover, the FEM calculation showed that the influence of the tail void on the total settlements is very small. As other factors influencing the settlements overshadow the effect of the tail void, it is impossible to directly relate the tail void induced settlements in a change in settlements.

However, when comparing the settlements of close locations, ruling out the influence of a changing geology, the tail void behaviour can be isolated. This showed that an increase in grout volume resulted in a better performing tail void, for the pressure no such relation was found. Theoretically this makes sense: a completely empty tail void would of course cause more settlements as (even an partly) a filled tail void, as the soil would move into the empty tail void en cause settlements at the surface. A real life example of an insufficiently filled tail void can be found in the case of the Jubilee line extension in London. Here, too little grout was used due to the slow response of the London clay, which lead to enormous long-term settlements due to the clay moving into the empty tail void (Kaalberg 2020). However, the soft soils in Amsterdam are not comparable with the stiff, slow responding London clay. In Amsterdam, the soil will react instantaneously, making it difficult to put the grout in place in time. Until the tail void is sufficiently filled with grout, the pressure of the grout can 'carry' the surrounding soil and keep the tail void opened. As long as the grout pressure is higher than the soil pressure, the soil is not expected to move into the tail void.

Something that supports the theory that the grout pressure stops the soil from moving into the tail void is the fact that under the frozen soil canopy, the grout pressure in the tail void showed to be lower than on any other location. Under this frozen canopy, the soil cannot move into the tail void. If the grout is loaded with the surrounding soil, the pressure of the grout would increase. This movement of the soil can be better explained with the help of a cafetière or French press¹. The soil is a porous medium just like the piston of the cafetière. The piston of the cafetière can not be pushed down instantaneously, first the water has to flow through the filter. The pressure on the piston will instead result in an increase of the fluid pressure underneath the piston. Alike this example, soil increases the pressure of the grout and will be slowed down from moving into the tail void.

After the TBM left the frozen canopy for the first time very large settlements occurred. As a result the TBM operators watched the grout injection process very closely and during the construction of the North/South line the grout pressure only fell below the soil pressure during TBM stand still when the tail void was already filled with grout. A fully filled tail void means that the particles in the grout, which volume is as big as 97% of the grout volume, can keep the surrounding soil from moving into the tail void. In the analogy of the French press this would mean that the beaker would be totally filled with ground coffee making it impossible to push the piston down. Overall the tail void is expected to have been filled very well over the North/South line project. This was confirmed by the locations where the cross paths were created between the tunnel tubes. Here, the lining was removed to create a pathway to the other tunnel tube. During this construction, the hardened grout could be observed and the tail void seemed to be filled fairly well. Additionally, chapter 2 showed the tail void tests performed before the boring of the North/South line. Here, a TBM that started too late with grouting was simulated. It started to move, causing the grout pressures to drop while the tail void was not yet filled with grout. The simulation showed that the soil filled up the tail void at that location.

9.3. Conclusions

The objective of this thesis was to gain a better understanding of the settlements induced by the tail void behind the TBM and on how the grouting of the tail void reduces the induced settlements. Before answering this main question, the sub questions as formulated in chapter 1 will be answered here.

How do the settlements develop during the passing of the TBM and which part of the settlements is affected by the tail void?

As was explained in chapter 2, the settlements induced by the TBM can be separated in four different phases: the settlements induced by the front, by the shield, by the tail void and those induced by consolidation. The settlements induced by the first three phases occur instantaneously, whereas the settlements induced by consolidation occur on the long term. Since, the third phase (the tail void) causes the last set of short-term settlements, the normalised settlement development curves as developed in this thesis (chapter 5) can be

¹A cafetière or French press is a coffee brewing device where coffee and hot water are put in a high cylindrical beaker. After brewing, a piston containing a filter is pushed down to separate the coffee ground and the brewed coffee.

used to identify the effect of the tail void on the settlements. These curves illustrate that the settlements induced by the tail void occur from the moment where the front of the TBM has passed approximately the 10 meter mark until approximately the 30 meter mark.

Can a relation be found between the injected grout volumes and the settlements induced by the tail void?

Yes, the analyses in chapter 4 illustrated that at the locations where lower grout volumes were used the tail void induced more settlements. This also makes sense from a theoretical point of view, as an empty tail void will cause soil to move towards the void, leading to settlements at the surface. For a fully filled tail void, the surrounding soil is less expected to move, therefore causing less settlements.

Can a relation be found between the grout pressures and the settlements induced by the tail void?

No, the data presented in chapters 4 and 5 show too much variation on this subject, making it impossible to find a general trend. Whereas the settlements induced by the tail void sometimes decrease as the grout pressure increases, the data also shows occurrences in which an increased grout pressure co-insists with increasing settlements.

How do the grout pressures develop over time i.e. do they dissipate when grout injections stops?

The different boring phases of the TBM can be recognised in the data from the grout pressures (chapter 7). When the TBM is boring and pushing itself forward, the tail void is filled with grout and the grout pressure increases. As the TBM stops to build up the tunnel rings, the injection of grout stops. As a consequence, the grout pressure drops over time. The speed of this dissipation depends on the permeability of the surrounding soil and the initial grout pressure. Furthermore, the data showed that during the boring of the start of the first trajectory, where the canopy was frozen, the grout pressure remained lower than at other locations where this was not the case. The fact that the soil is frozen prevents the soil from moving into the tail void. This shows that the soil pressure around the tail void also plays a factor on the grout pressure in the tail void.

Main question: *To what extend is the tail void behind the TBM responsible for the settlements and does the grouting of this tail void reduce these settlements?*

As the settlements induced by the different components of the TBM overlap in the data, it is impossible to quantify the contribution of the tail void for the settlements. However, comparing the data of two nearby locations the performances of both tail voids can be compared.

A better performing tail void under similar TBM behaviour will have a relatively smaller contribution on the total settlements than an under performing tail void. As chapters 4 and 5 illustrate that the use of a larger grout volume enhances the performance of the tail void, it can be concluded that a sufficient filling of the tail void can reduce the settlements.

Recommendations

Optimal grout volume

In this thesis it was concluded that a well performing tail void can reduce settlements. The grout volume injected in the tail void is one of the factors affecting the performance of the tail void. It is therefore recommended to conduct further research on the optimal volume for the grout fill of the tail void. Note that this is possibly effected by the surrounding soil and can therefore vary within a project.

Fill grade of the tail void

Above recommendation showed that the optimal grout volume in the tail void varies with the surrounding soil. Therefore, it would be nice to have a method to check the fill grade during drilling. It can be expected that when the tail void is getting fuller it gets more difficult to inject more grout. This could be used to develop a measure for a sufficient filled tail void.

Limitations of the data and assumptions made

In order to perform the analyses of Chapter 4, the assumption was made that the for every data point, the first measurement would represent the 0 settlement. The value of this measurement was subtracted from all other measurements to determine the settlement per data point, over time. However, this does not take into account the background settlements of the surrounding soil, induced by other factors than the TBM itself. When the maximum influence of the TBM is known this could be used to chose a 0 closer to the moment the TBM passes, decreasing the influence of the background settlements.

Further appliance of the normalised settlement curves

The normalised settlement curves as developed in this thesis to assess the performance of the tail void, could be a useful tool in many other appliances. Example could be the assessment of the performance of other parts of the TBM, possibly even on site during the tunnel boring.

Influence of the soil on the grouting pressures

One of the conclusions of this thesis was that the soil pressure influences the grout pressure. As the focus of the thesis was the influence of the grout pressure on the soil and its settlements, this is not researched any further. To further support this conclusion the influence of the ground pressures can be investigated further.

Improving (normalised) settlement development curves

To compare two different settlement development curves one could subtract one from the other. This way the difference is shown and it can directly be seen where one graph is performing different from the other. In this research this is not used because the idea did not come up untill the end of the research.

Bibliography

- P.B. Attewell, J. Yeat, and A.R. Selby. Soil Movements Induced by Tunneling and Their Effects on Pipelines and Structures. 1986.
- S. Babendererde. Grouting the shield tail gap. *Tunnels & Tunneling International*, 31(11):48–49, nov 1999. URL www.tunnelsonline.info/features/grouting-the-shield-tail-gap/.
- A. Bezuijen and K.J. Bakker. The influence of flow around a TBM machine. In *6th Int. Symposium on Geotech. Aspects of Underground Construction in Soft Ground int.*, number January, Shanghai, 2008. ISBN 9780415484756. doi: 10.1201/9780203879986.ch29.
- A. Bezuijen and A. Talmon. Processes around a TBM. *Geotechnical Aspects of Underground Construction in Soft Ground*, 3(GeoInternational):48–56, 2008. doi: 10.1201/9780203879986.ch1.
- A. Bezuijen and A.M. Talmon. Grout, the foundation of a bored tunnel. In Thomas Telford, editor, *Proc. BGA. Int. Conf. Foundations(ICOF)*, Dundee, 2003. doi: 10.1201/9781439834268.ch14.
- A. Bezuijen, F. Nagel, and G. Mechke. Flow around a TBM: A Comparison of analytical and numerical models. In G. Viggiani, editor, *Geotechnical Aspects of Underground Construction in Soft Ground*, pages 173–179, Rome, 2011. Taylor & Francis Group.
- COB. Amsterdam, Noord/Zuidlijn. URL <https://www.cob.nl/over-ondergronds-bouwen/voorbeeldprojecten/amsterdam-noordzuidlijn/>.
- COB. Monitoring in de praktijk: Ervaringen grote infraprojecten. Technical report, COB, 2016. URL <https://www.cob.nl/document/monitoring-in-de-praktijk/>.
- D. Cook, R. de Bakker, Nijs, and S. Frankenmolen. Amsterdam Noord/Zuidlijn: Use of Background Monitoring Data Prior to Construction Commencement. In *FMGM 2007: Field Measurements in Geomechanics*, number September, Boston, Massachusetts, 2007. ISBN 9780784409404.
- T.G.S. Dias and A. Bezuijen. TBM Pressure Models - Observations, Theory and Practice. *Pcsmge 15 2015*, (November):347–374, 2015. doi: 10.3233/978-1-61499-599-9-347. URL http://ebooks.iospress.nl/volumearticle/41347{%}5Cnhttps://www.researchgate.net/publication/283855639_{_}TBM_{_}Pressure_{_}Models_{_}{_}Observations_{_}Theory_{_}and_{_}Practice.
- T.G.S. Dias and A. Bezuijen. Grout pressure distribution during TBM tunnelling. *Geotechnical Aspects of Underground Construction in Soft Ground*, (April 2017):153–160, 2017. doi: 10.1201/9781315099507-17.
- B.F.J. Dijk van and F.J. Kaalberg. 3-D Geotechnical Model for the North/Southline in Amsterdam. In A. Civini, editor, *Application of Numerical Methods to Geotechnical Problems*, pages 739–749. Springer-Verlag, Vienna, 1998. ISBN 978-3-7091-2512-2. doi: 10.1007/978-3-7091-2512-0_71. URL http://link.springer.com/10.1007/978-3-7091-2512-0_{_}71.
- D. Festa. *On the Interaction between a Tunnel Boring Machine and the Surrounding Soil*. PhD thesis, TU Delft, 2015.
- T.K. Haji. *Evaluating the Effects of Tunnel Construction on Buildings*. PhD thesis, The University of Nottingham, 11 2017.
- F. J. Kaalberg. personal communication, 2020.
- F. J. Kaalberg, E. Teunissen, F. Tol, and J. Bosch. Dutch research on the impact of shield tunnelling on pile foundations. 16, 03 2006. doi: 10.1201/NOE0415391245.ch13.

- E. J. Kaalberg, N. C. Empel van, P. P. M. K. Janssen, and J. F. W. Joustra. North / South line Amsterdam, Tunnelling close to Piled Foundations: TBM Design, Settlement Performance, Compensation Grouting, Injactable Coupling System for the Tunnelrings. In *STUVA*, Berlin, 2011.
- E.J. Kaalberg and V. Hentschel. Tunnelvortrieb in weichen Böden mit hohem Wasserstand zur Entwicklung einer setzunsorientierten un setzungsminimierenden Betriebsweise der TBM. [Tunnel boring in soft soils with a high water level, development of a settlement oriented and settlement minimizing TBM control.]. *Forschung und Praxis*, 31(37):48–49, 1998.
- E.J. Kaalberg, J. Haasnoot, and H. Netzel. What are the end-user issues? Settlement risk management in underground construction. In *New Paradigms in Subsurface Prediction*, volume 99 of *Lecture Notes in Earth Sciences*, pages 69–83. Springer Berlin Heidelberg, Berlin, Heidelberg, 2003. ISBN 978-3-540-48019-8. doi: 10.1007/3-540-48019-6_6. URL http://link.springer.com/10.1007/3-540-48019-6_6.
- S. Möller. *Tunnel induced settlements and structural forces in linings*. PhD thesis, Universität Stuttgart, Mitteilung 54 des Instituts für Geotechnik, 6 2006.
- R.B. Peck. Deep excavations and tunnelling in soft ground. *Proc. Of the seventh intern. conf. on Soil Mechanics and Foundation Engineering, Mexico*, 1969.
- K.J. Reinders. *Reader CIE 5305 Bored and Immersed Tunnels*. TU Delft, Delft, 1 edition, 2018.
- M.N. Vu, W. Broere, and J. Bosch. Volume loss in shallow tunnelling. *Tunnelling and Underground Space Technology*, 2016. ISSN 08867798. doi: 10.1016/j.tust.2016.06.011.